

**Supplementary Information for
Investigating the effect of alumina shaping on the
sorption properties of promising metal-organic
frameworks**

Paul Iacomi^a, U-Hwang Lee^{b,c}, Anil H. Valekar^{b,c}, Jong-San Chang^{b,d}, and Philip L. Llewellyn^{a,*}

^aAix-Marseille Université, CNRS, MADIREL UMR 7246, 13397 Marseille, France

^bResearch Group for Nanocatalysts, Korea Research Institute of Chemical Technology (KRICT), Daejeon 305–600, Korea

^cDepartment of Green Chemistry, University of Science and Technology (UST), 217 Gajeong-Ro, Yuseong, Daejeon 305–350, Korea

^dDepartment of Chemistry, Sungkyunkwan University, Suwon 440–476, Korea

* *philip.llewellyn@univ-amu.fr*

1. Material synthesis procedure

1.1. UiO-66(Zr). The scaled-up synthesis of UiO-66(Zr) was carried out in a 5 L glass reactor (Reactor Master, Syrris, equipped with a reflux condenser and a Teflon-lined mechanical stirrer) according to a previously reported method.^{S1} In short, 462 g (2.8 mol) of H₂BDC (98%) was initially dissolved in 2.5 L of DMF (2.36 kg, 32.3 mol) at room temperature. Then, 896 g (2.8 mol) of ZrOCl₂ · 8 H₂O (98%) and 465 mL of 37% HCl (548 g, 15 mol) were added to the mixture. The molar ratio of the final ZrOCl₂ · 8 H₂O/H₂BDC/DMF/HCl mixture was 1:1:11.6:5.4. The reaction mixture was vigorously stirred to obtain a homogeneous gel. The mixture was then heated to 423 K at a rate of 1 K min⁻¹ and maintained at this temperature for 6 h in the reactor without stirring, leading to a crystalline UiO-66(Zr) solid. The resulting product (510 g) was recovered from the slurry by filtration, redispersed in 7 L of DMF at 333 K for 6 h under stirring, and recovered by filtration. The same procedure was repeated twice, using MeOH instead of DMF. The solid product was finally dried at 373 K overnight.

1.2. MIL-100(Fe). The synthesis of the MOF for the shaping study was done at the KRICT institute using a previously published method.^{S2} To synthesise the MIL-100(Fe) material Fe(NO₃)₃ was completely dissolved in water. Then, BTC was added to the solution; the resulting mixture was stirred at room temperature for 1 h. The final composition was Fe(NO₃)₃ · 9 H₂O:0.67 BTC:*n*H₂O (*n*= 55–280). The reactant mixture was heated at 433 K for 12 h using a Teflon-lined pressure vessel. The synthesized solid was filtered and washed with deionized (DI) water. Further washing was carried out with DI water and ethanol at 343 K for 3 h and purified with a 38 mM NH₄F solution at 343 K for 3 h. The solid was finally dried overnight at less than 373 K in air.

1.3. MIL-127(Fe). MIL-127(Fe) was synthesized by reaction of Fe(ClO₄)₃ · 6 H₂O (3.27 g, 9.2 mmol) and C₁₆N₂O₈H₆ (3.3 g) in DMF (415 mL) and hydrofluoric acid (5 M, 2.7 mL) at 423 K in a Teflon flask. The obtained orange crystals were placed in DMF (100 mL) and stirred at ambient temperature for 5 h. The final product was kept at 375 K overnight. MIL-127(Fe) was synthesized by reaction of Fe(ClO₄)₃ · 6 H₂O (3.27 g, 9.2 mmol) and C₁₆N₂O₈H₆ (3.3 g) in DMF (415 mL) and hydrofluoric acid (5 M, 2.7 mL) at 423 K in a Teflon flask. The obtained orange crystals were placed in DMF (100 mL) and stirred at ambient temperature for 5 h. The final product was kept at 375 K overnight.

2. Detailed experimental procedure for characterisation

2.1. Thermogravimetric analysis. TGA experiments were carried out on ca. 15 mg sample with a Q500 (TA Instruments) apparatus in a dynamic “Hi-Res” mode at a ramp of 3 K min^{-1} under both nitrogen and argon flow at $30\text{ cm}^3\text{ min}^{-1}$.

2.2. Bulk density measurements. Bulk density was determined by weighing 1.5 ml empty glass vessels and settling the MOF inside. Powder or pellet material is then added in small increments and settled through vibration between each addition. The full vessel is finally weighed, which allowed the bulk density to be determined. The same cell is used in all experiments, with cleaning through sonication between each experiment.

2.3. Sample activation for adsorption. The materials were pre-treated before all adsorption experiments by activation at high temperature under secondary vacuum for 16 hours. The activation temperature was set to 150 °C all materials.

2.4. Nitrogen physisorption at 77 K. Nitrogen adsorption experiments are carried out on a Micromeritics Triflex apparatus. Approximately 60 mg of sample are used for each measurement. Empty glass cells are weighed and filled with the samples, which are then activated in a Micromeritics Smart VacPrep up to their respective activation temperature under vacuum and then back-filled with an inert atmosphere. After sample activation, the cells are re-weighed to determine the precise sample mass. The cells are covered with a porous mantle which allows for a constant temperature gradient during measurement by wicking liquid nitrogen around the cell. Finally, the cells are immersed in a liquid nitrogen bath and the adsorption isotherm is recorded using the volumetric method. A separate cell is used to condense the adsorptive throughout the measurement for accurate determination of its saturation pressure. The BET area on these microporous solids was calculated using the procedure devised by Rouquerol *et al.*^{S3}. Accessible pore volume was calculated from the amount adsorbed at $p/p^0 = 0.8$.

2.5. Water adsorption at 298 K. Vapour adsorption isotherms throughout this work are measured using a MicrotracBEL BELSORP-max apparatus. Glass cells are first weighed and then filled with about 50 mg of sample. The vials are then heated under vacuum up to the activation temperature of the material and re-weighed in order to measure the exact sample mass without adsorbed guests. The cells are then immersed in a mineral oil bath kept at 298 K. To ensure that the cold point of the system occurs in the material and to prevent condensation on cell walls, the reference volume, dead space and vapour source are temperature controlled through an insulated enclosure.

2.6. Microcalorimetry at 303 K. Gas adsorption isotherms and differential enthalpies were measured using a Tian-Calvet type microcalorimeter coupled with a home-made manometric gas dosing system.^{S4} This apparatus allows the simultaneous measurement of the adsorption isotherm and the corresponding differential enthalpies. Gas is introduced into the system using a step-by-step method and each dose is allowed to stabilize in a reference volume before being brought into contact with the adsorbent located in the microcalorimeter. The introduction of the adsorbate to the sample is accompanied by an exothermic thermal signal, measured by the thermopiles of the microcalorimeter. The peak in the calorimetric signal is integrated to obtain the total energy released during an adsorption step. At low coverage the error in the signal can be estimated to around $\pm 0.2\text{ kJ mol}^{-1}$. Around 0.4 g of sample is used in each experiment. For each injection of gas, equilibrium was assumed to have been reached after 90 minutes. This was confirmed by the return of the calorimetric signal to its baseline ($<5\text{ }\mu\text{W}$). The gases used for the adsorption were obtained from Air Liquide and were of minimum N47 quality (99.997 % purity).

3. TGA curves

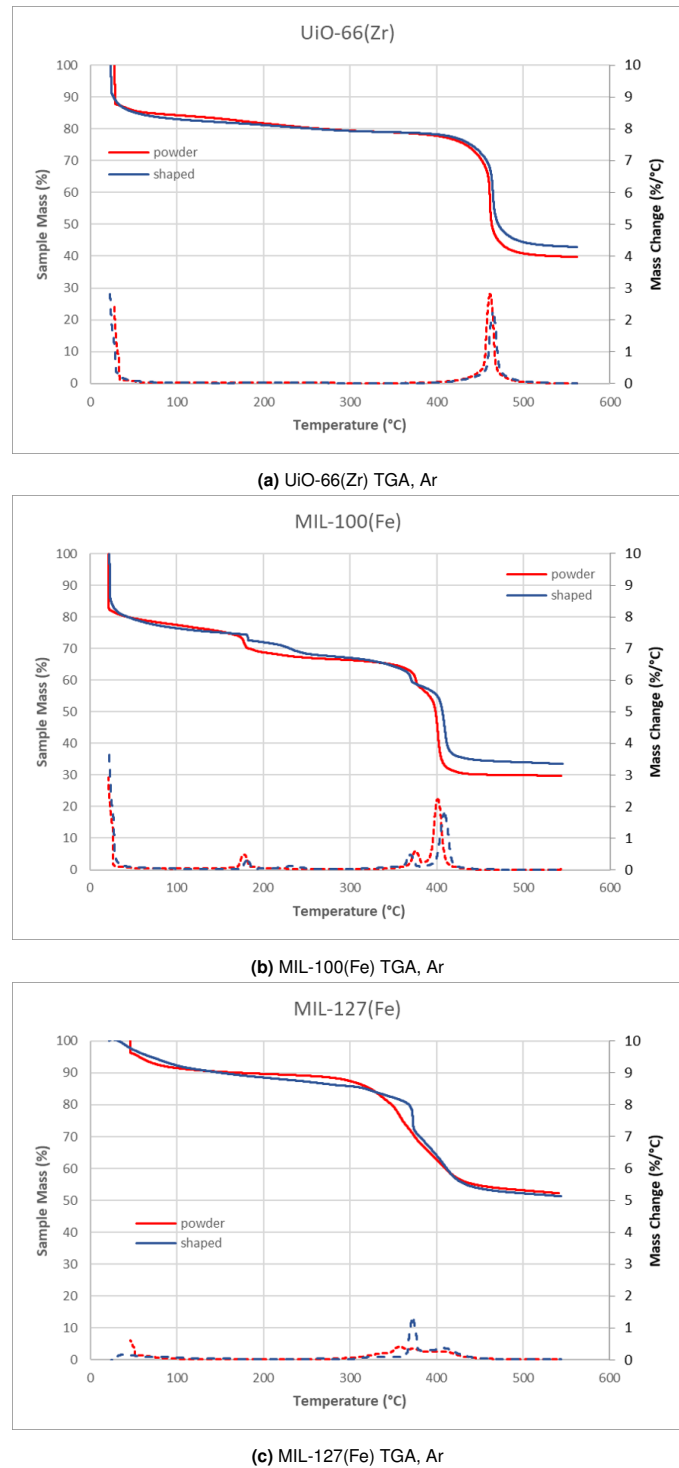


Fig. S1. TGA curves of investigated MOFs

4. Nitrogen physisorption at 77K

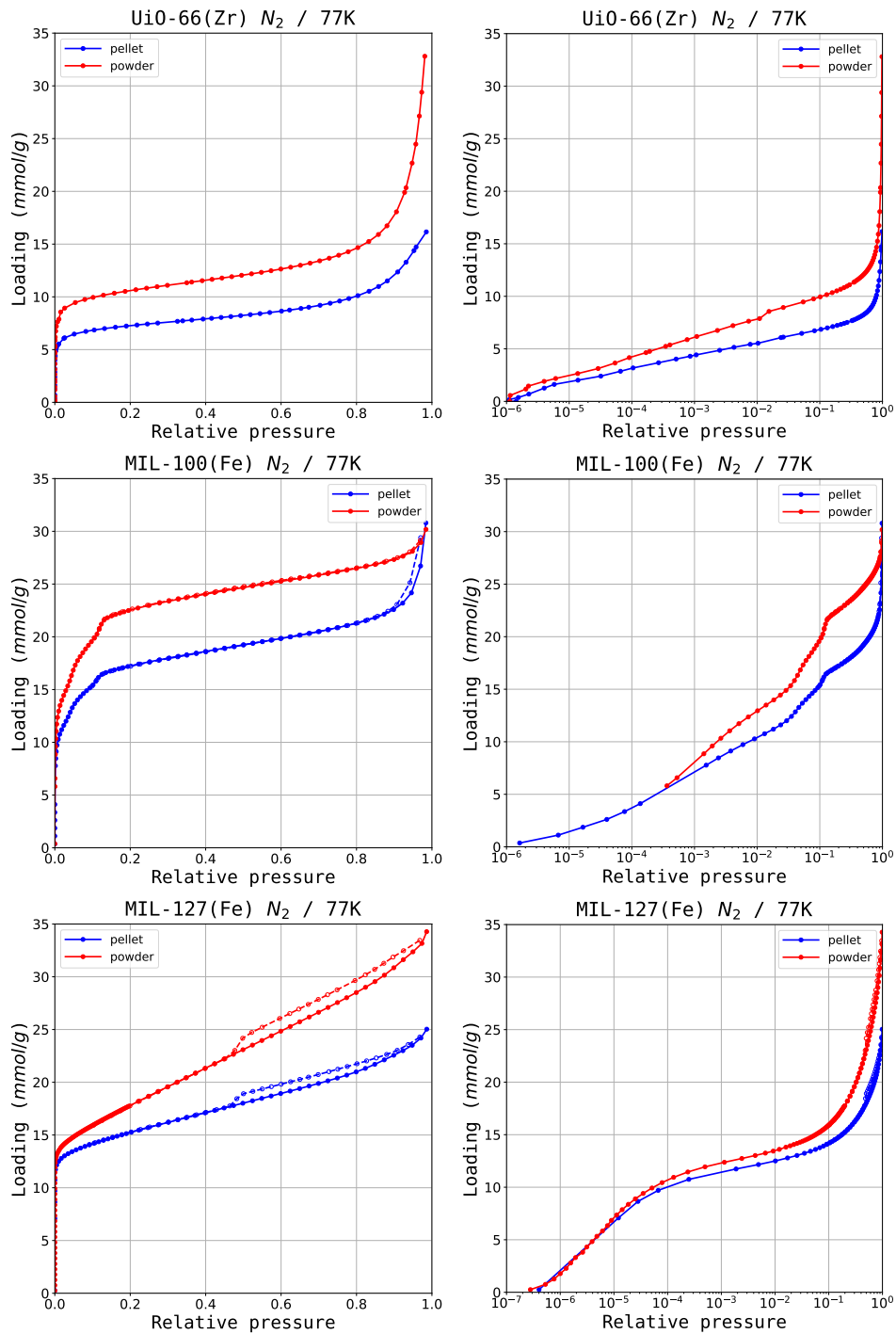


Fig. S2. Nitrogen at 77K adsorption isotherms measured on the shaped pellets (blue) and original powder (red).

5. Nitrogen physisorption at 77K after ambient exposure

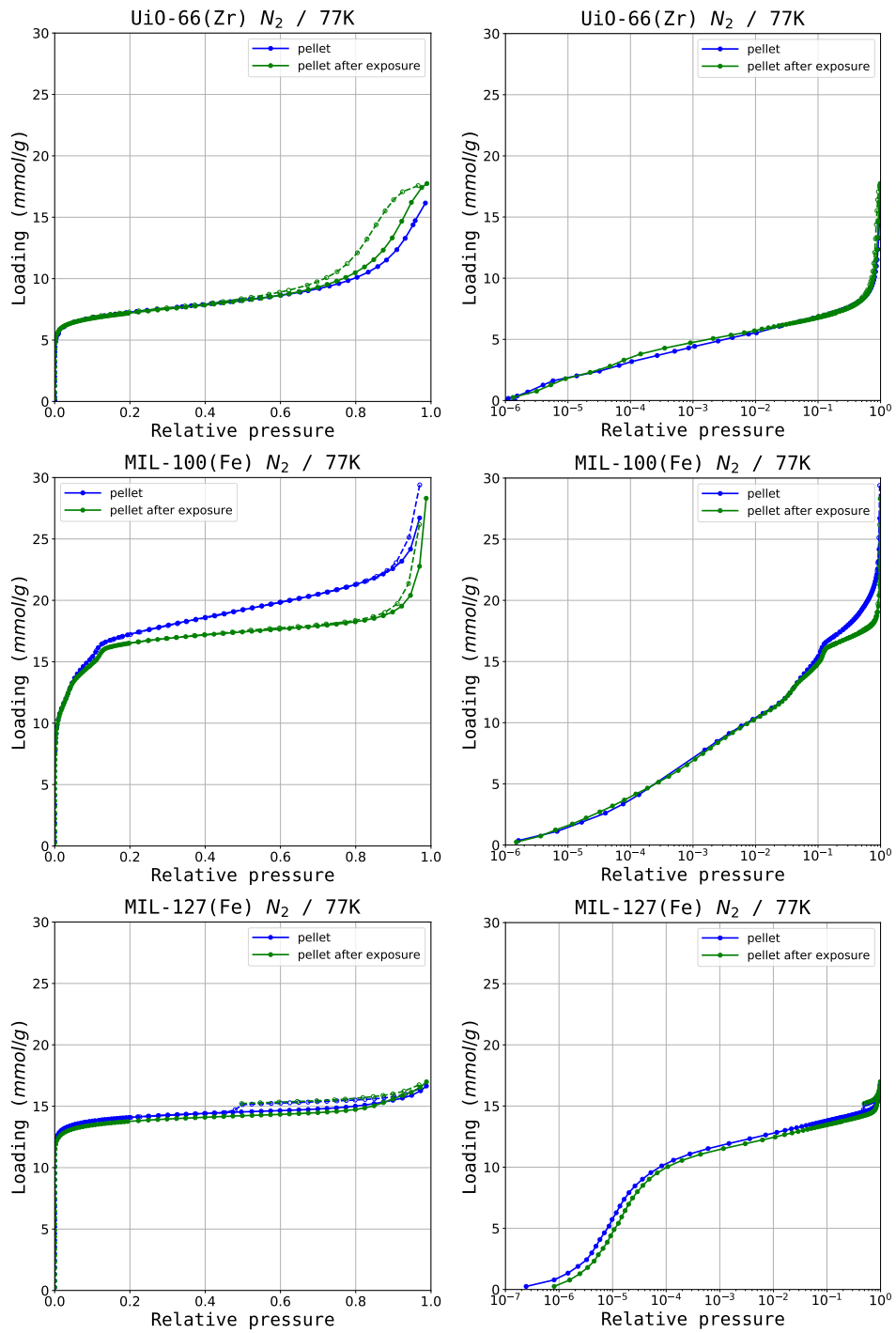


Fig. S3. Nitrogen at 77K adsorption isotherms measured on the shaped pellets before (blue) and after (green) exposure to ambient conditions.

6. Calorimetry dataset

Calorimetry UiO-66(Zr)

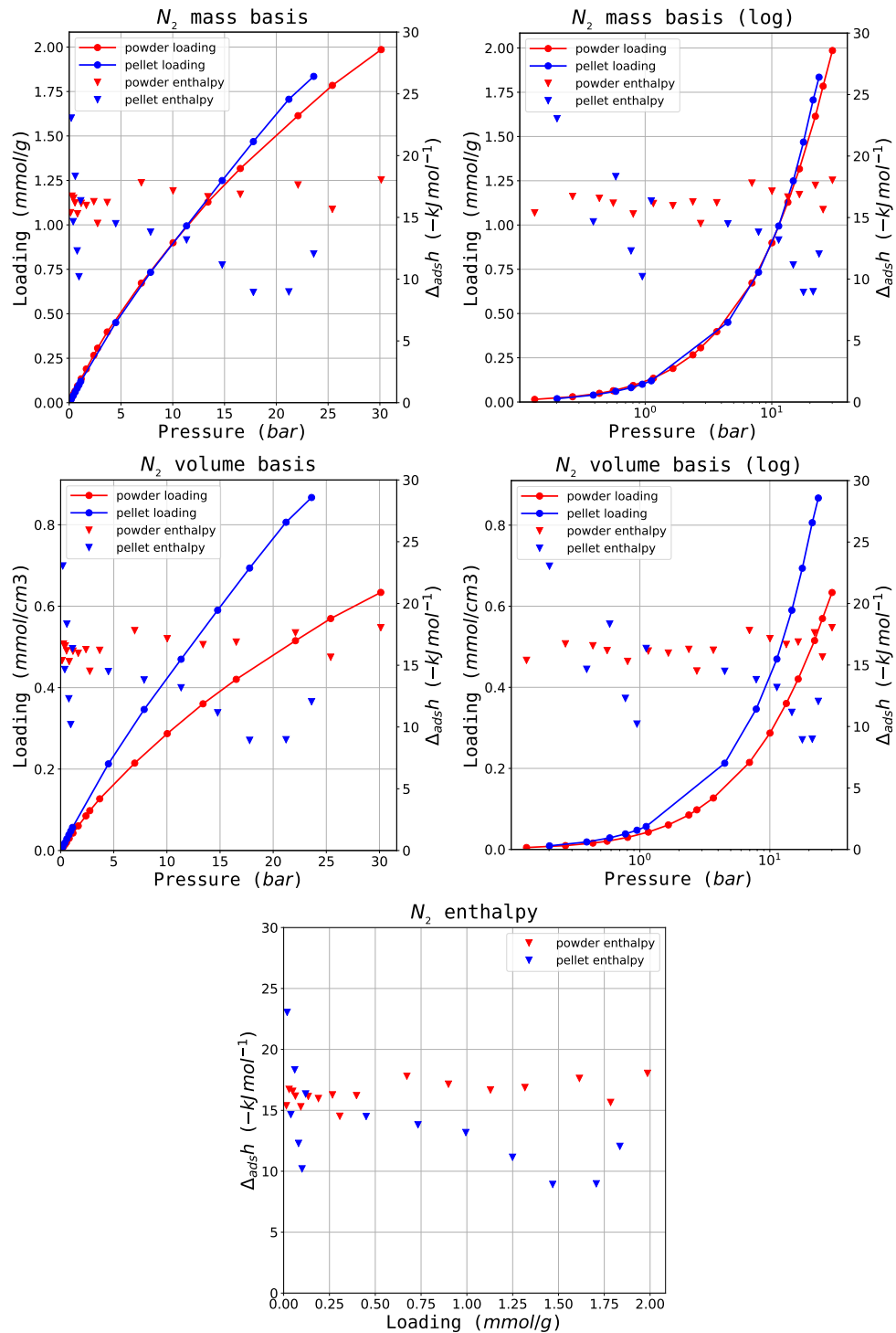


Fig. S4. Nitrogen calorimetric dataset for UiO-66(Zr)

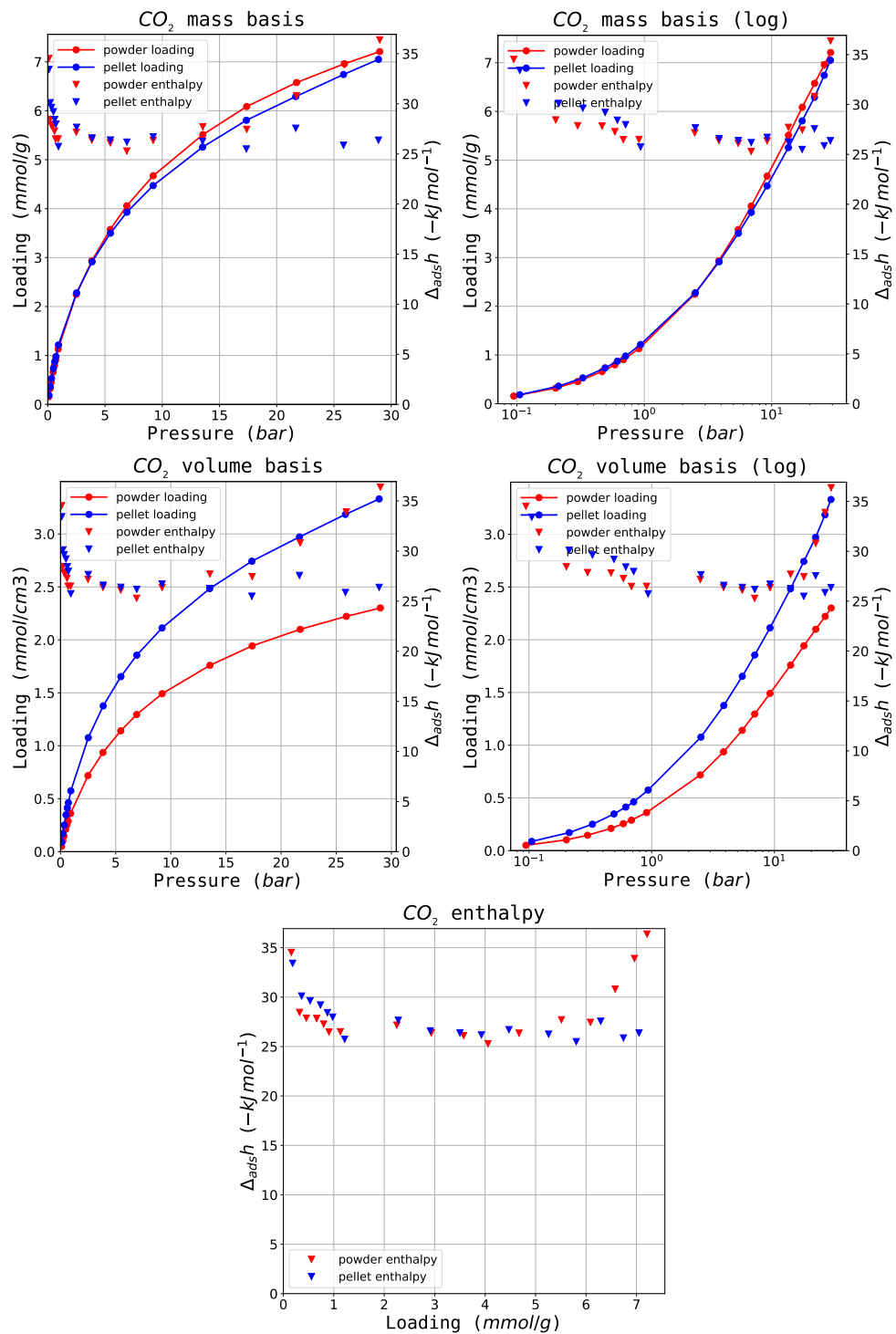


Fig. S5. Carbon dioxide calorimetric dataset for UiO-66(Zr)

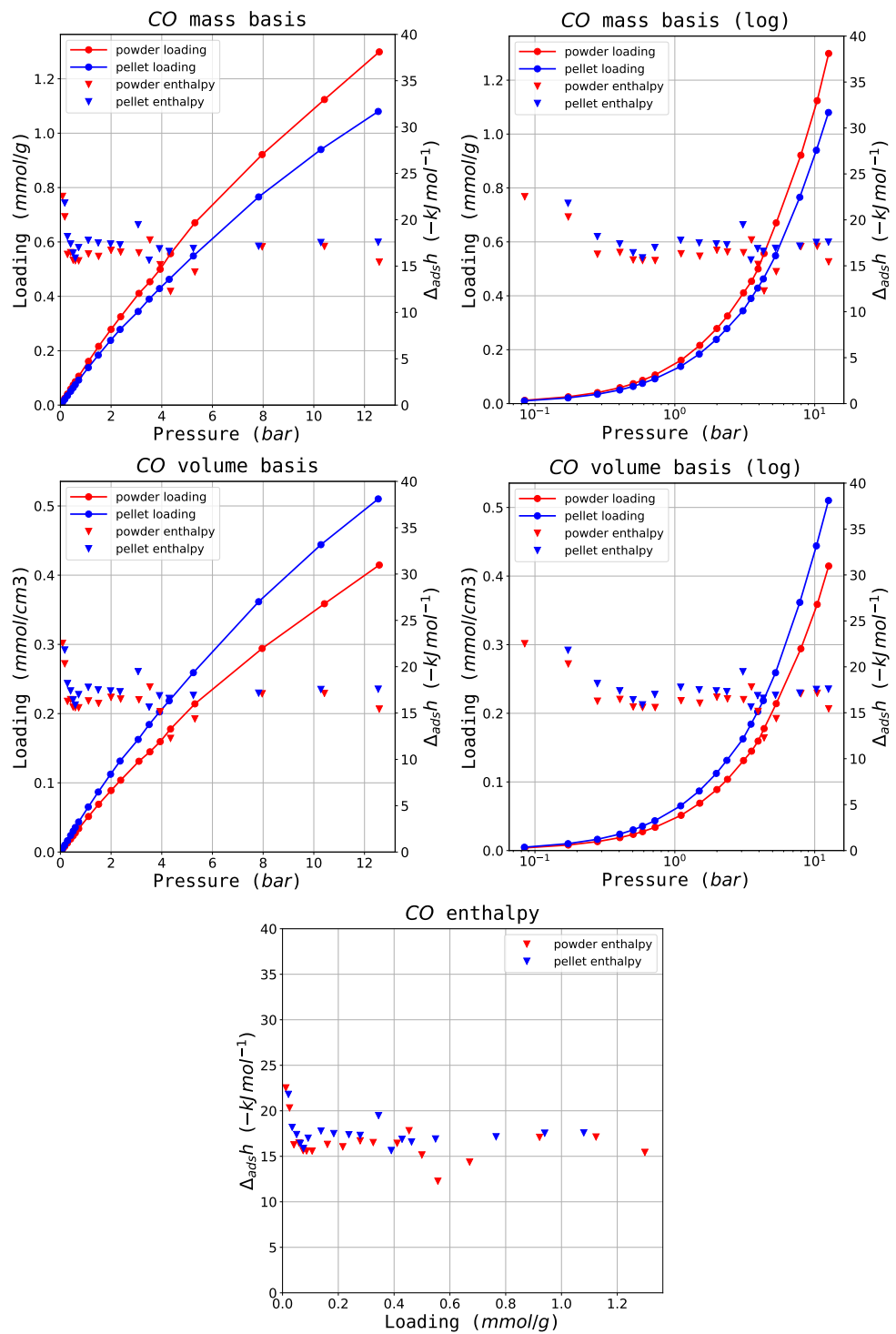


Fig. S6. Carbon monoxide calorimetric dataset for UiO-66(Zr)

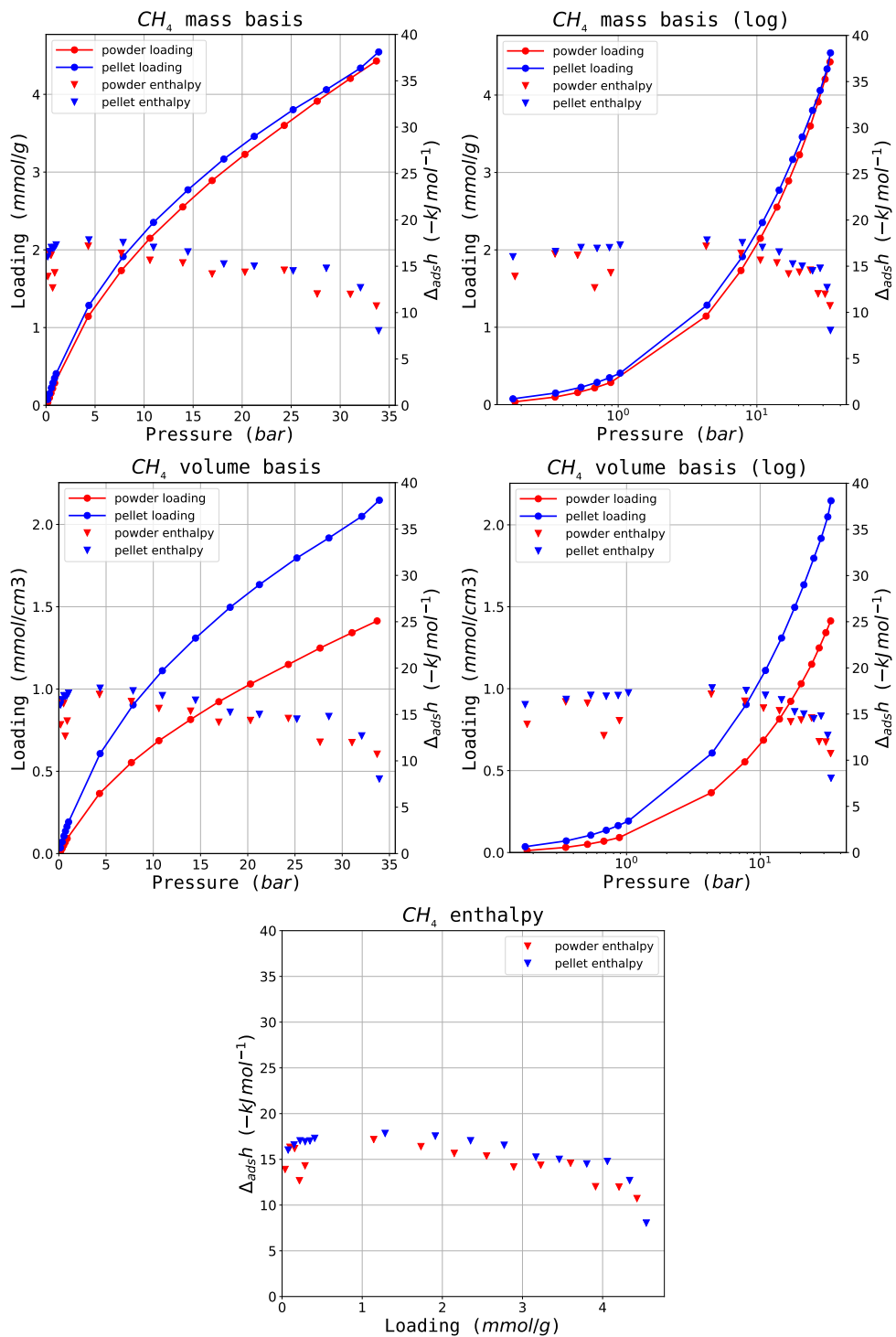


Fig. S7. Methane calorimetric dataset for UiO-66(Zr)

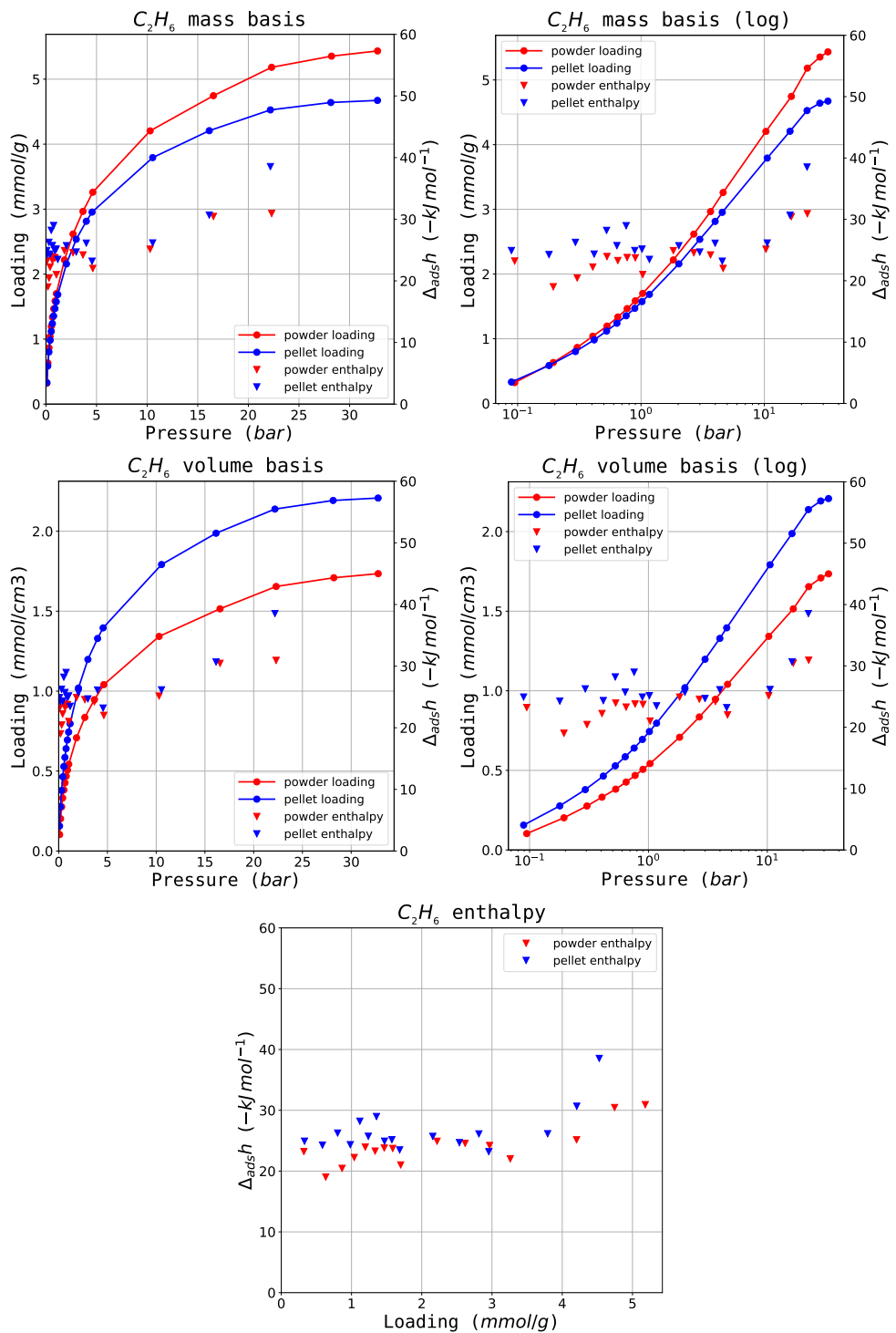


Fig. S8. Ethane calorimetric dataset for UiO-66(Zr)

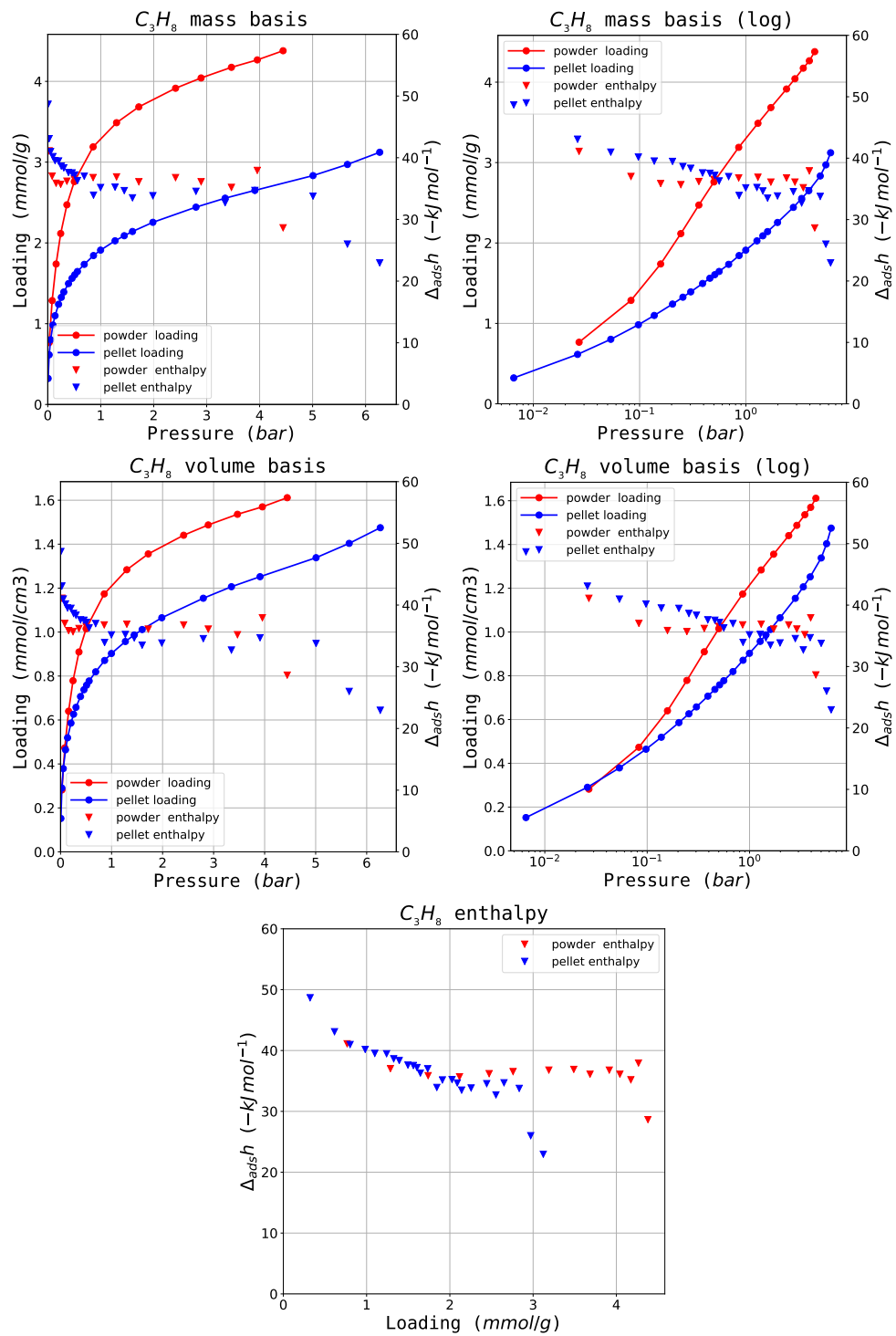


Fig. S9. Propane calorimetric dataset for UiO-66(Zr)

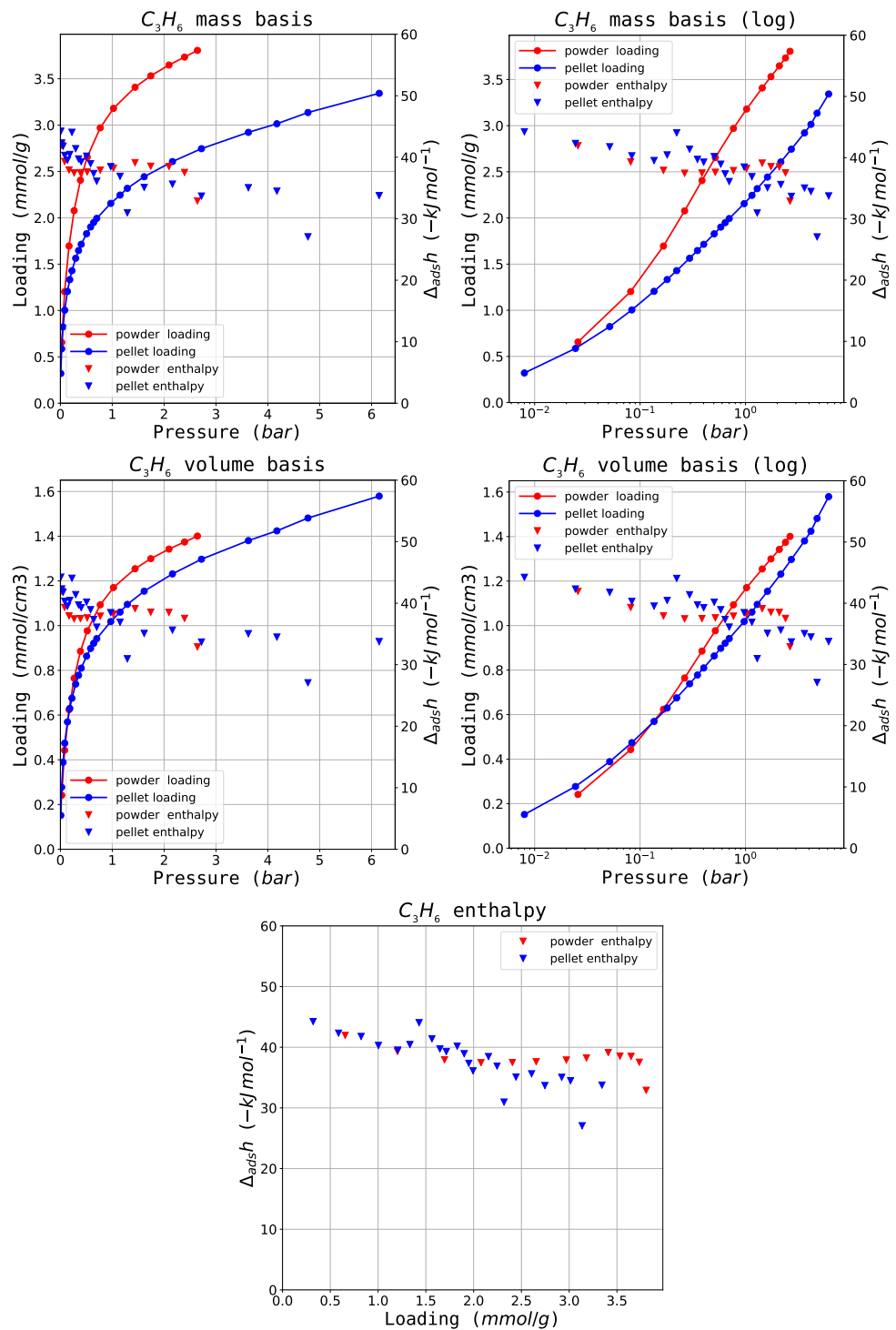


Fig. S10. Propylene calorimetric dataset for UiO-66(Zr)

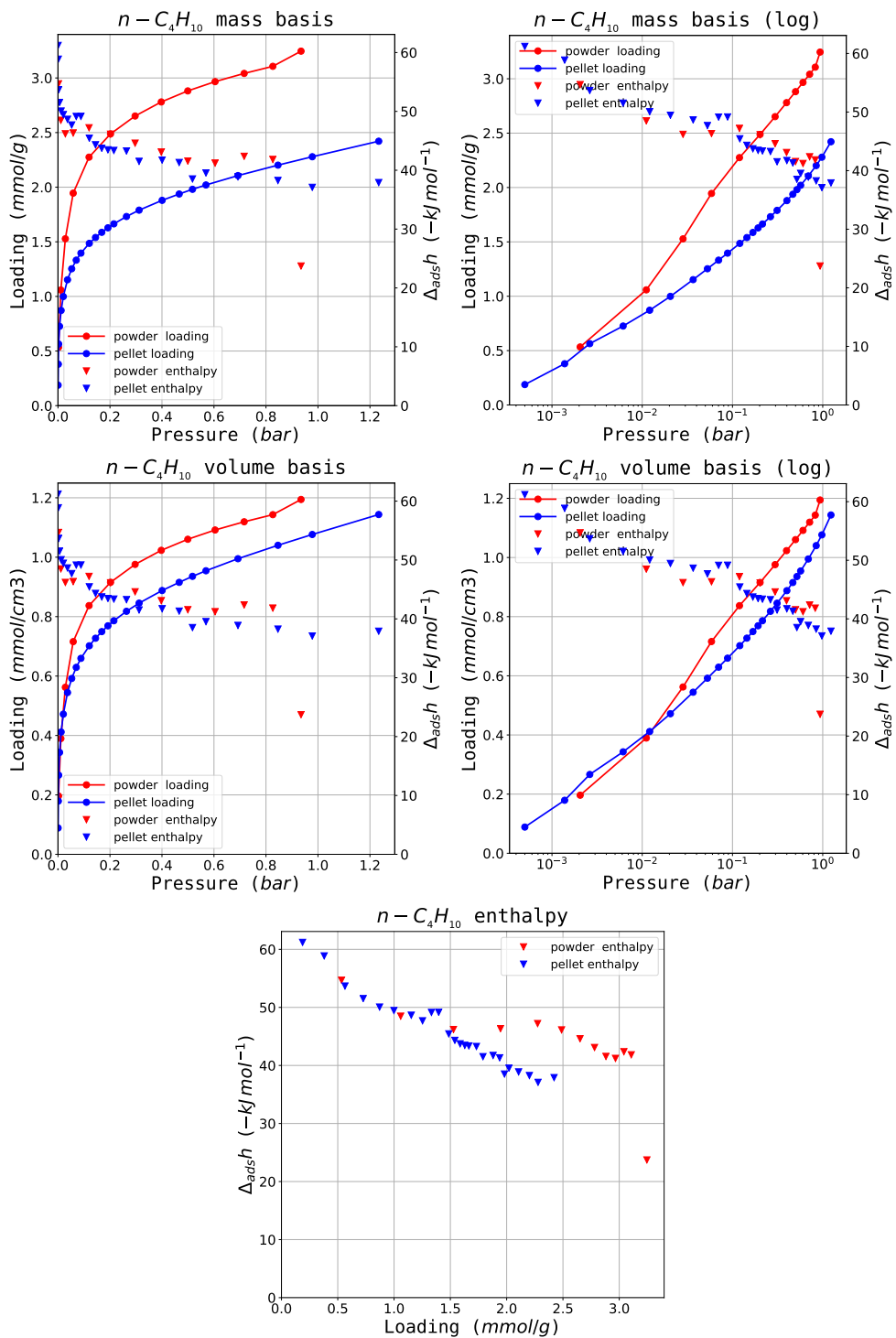


Fig. S11. Butane calorimetric dataset for UiO-66(Zr)

Calorimetry MIL-100(Fe)

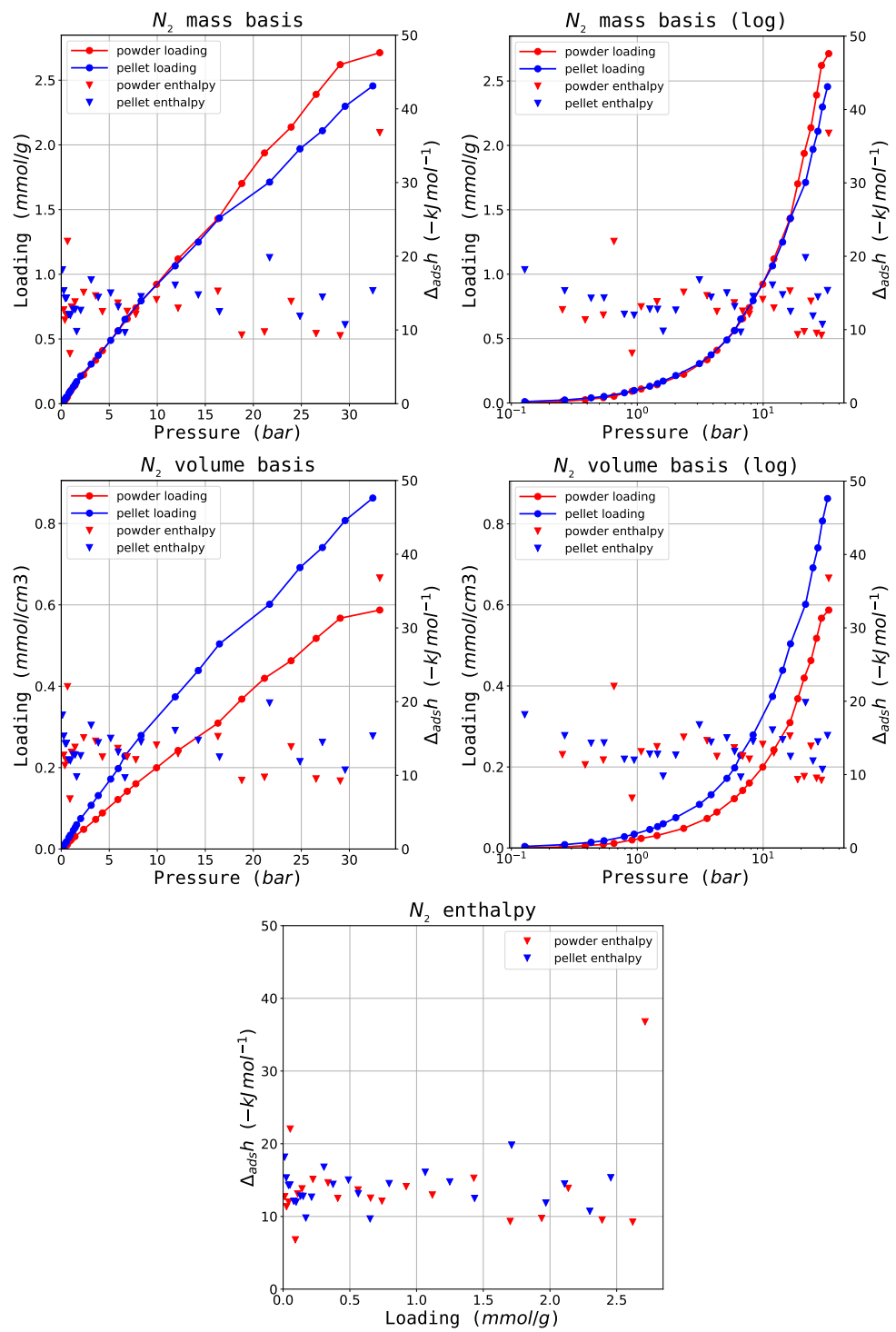


Fig. S12. Nitrogen calorimetric dataset for MIL-100(Fe)

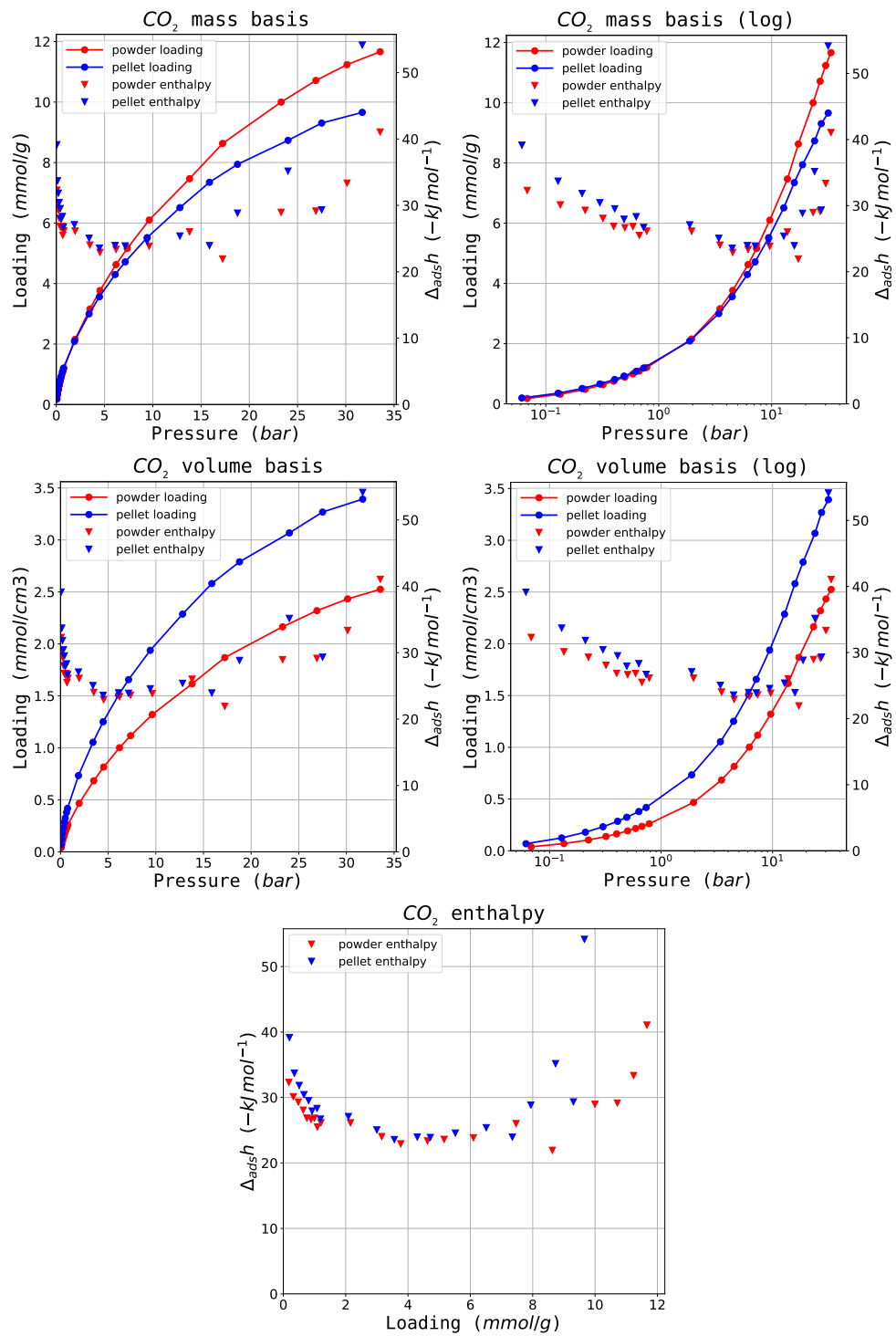


Fig. S13. Carbon dioxide calorimetric dataset for MIL-100(Fe)

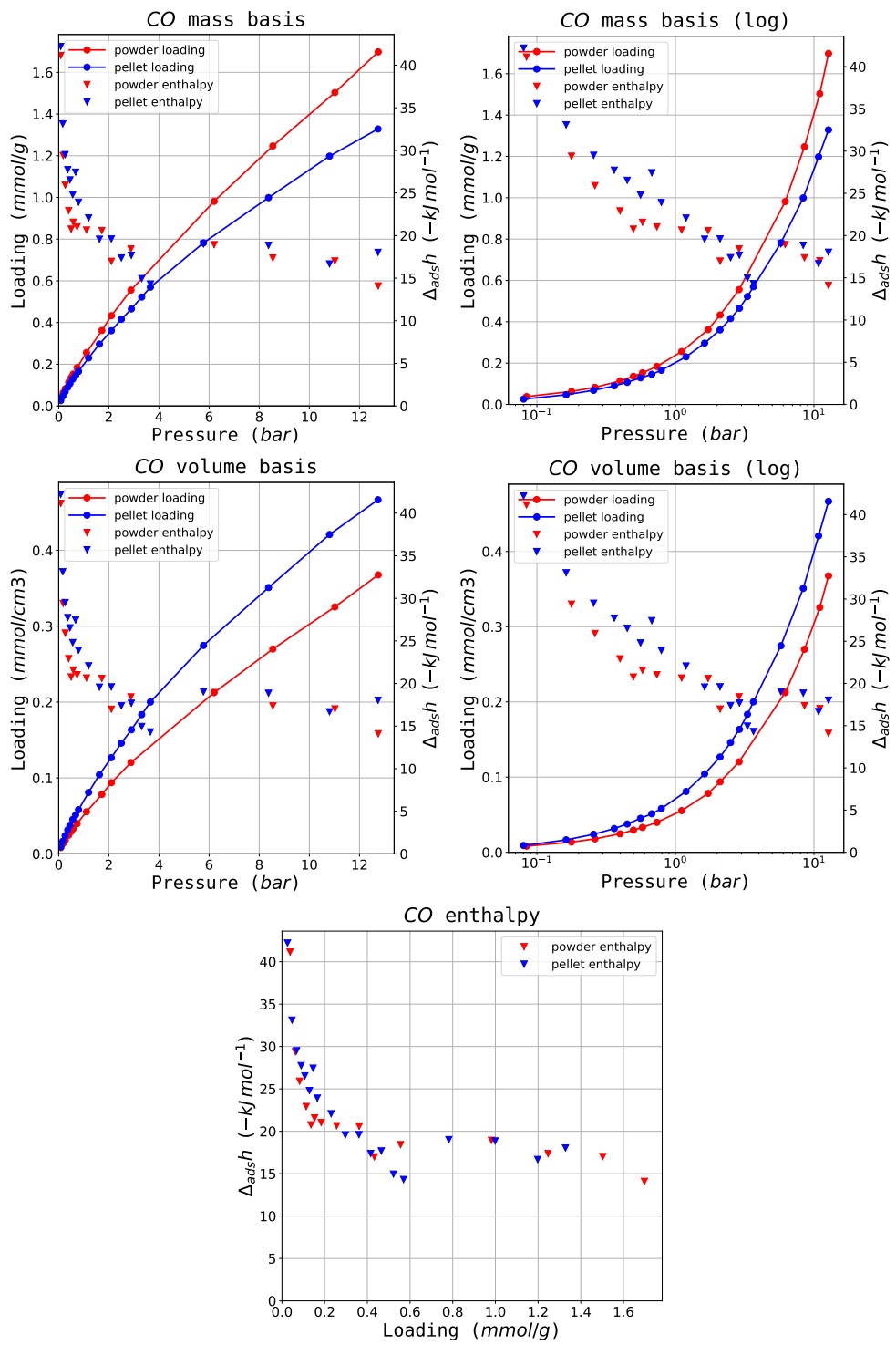


Fig. S14. Carbon monoxide calorimetric dataset for MIL-100(Fe)

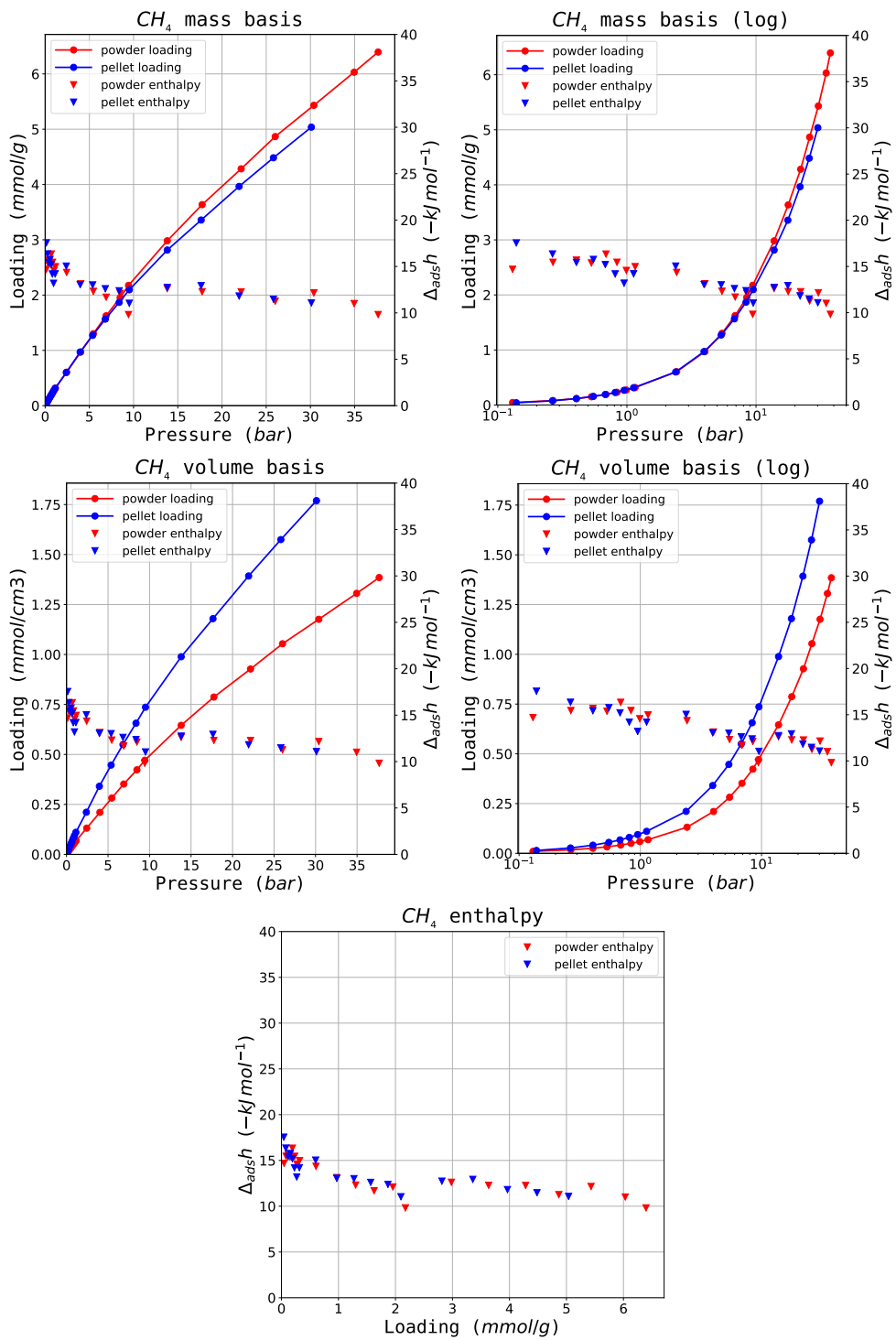


Fig. S15. Methane calorimetric dataset for MIL-100(Fe)

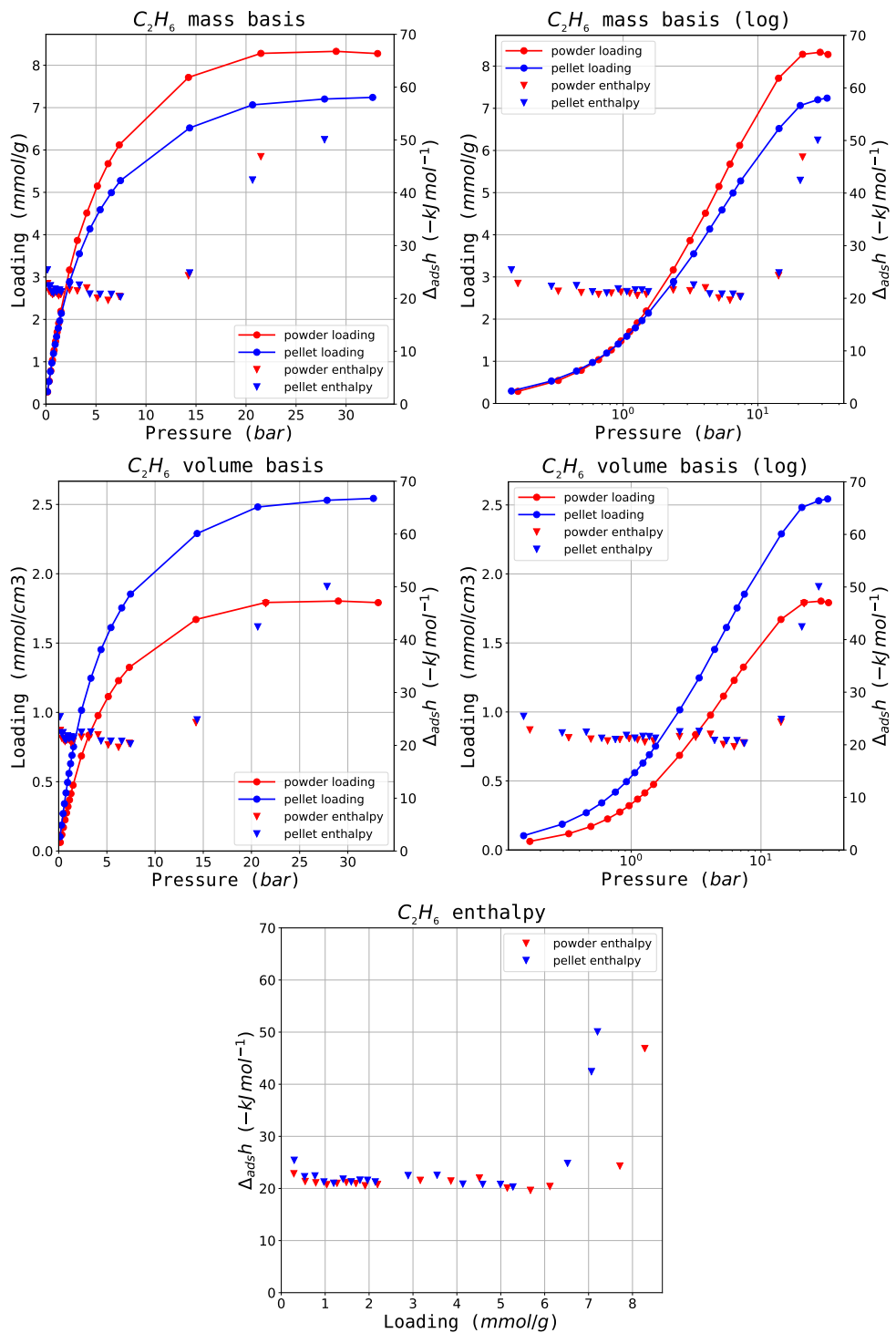


Fig. S16. Ethane calorimetric dataset for MIL-100(Fe)

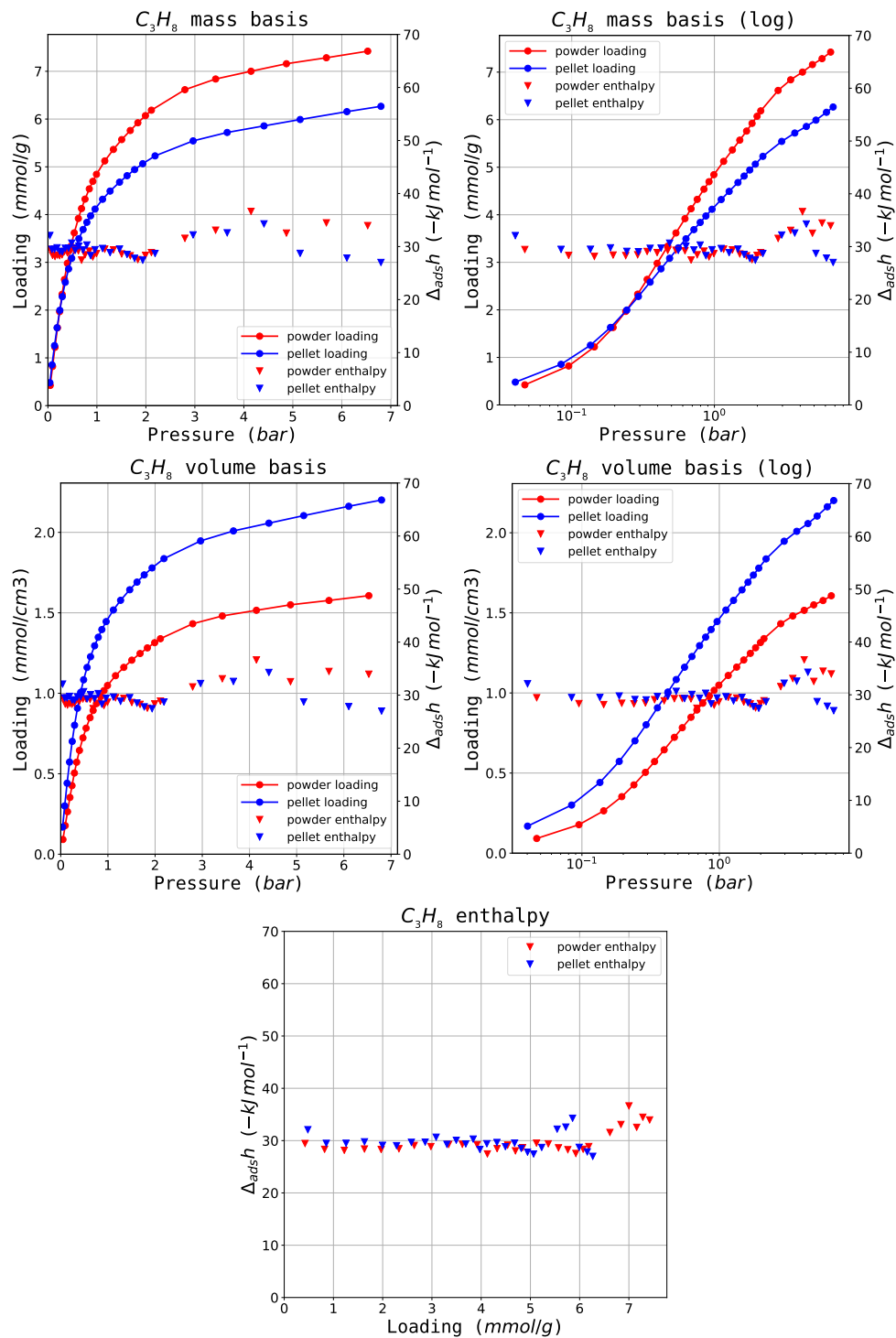


Fig. S17. Propane calorimetric dataset for MIL-100(Fe)

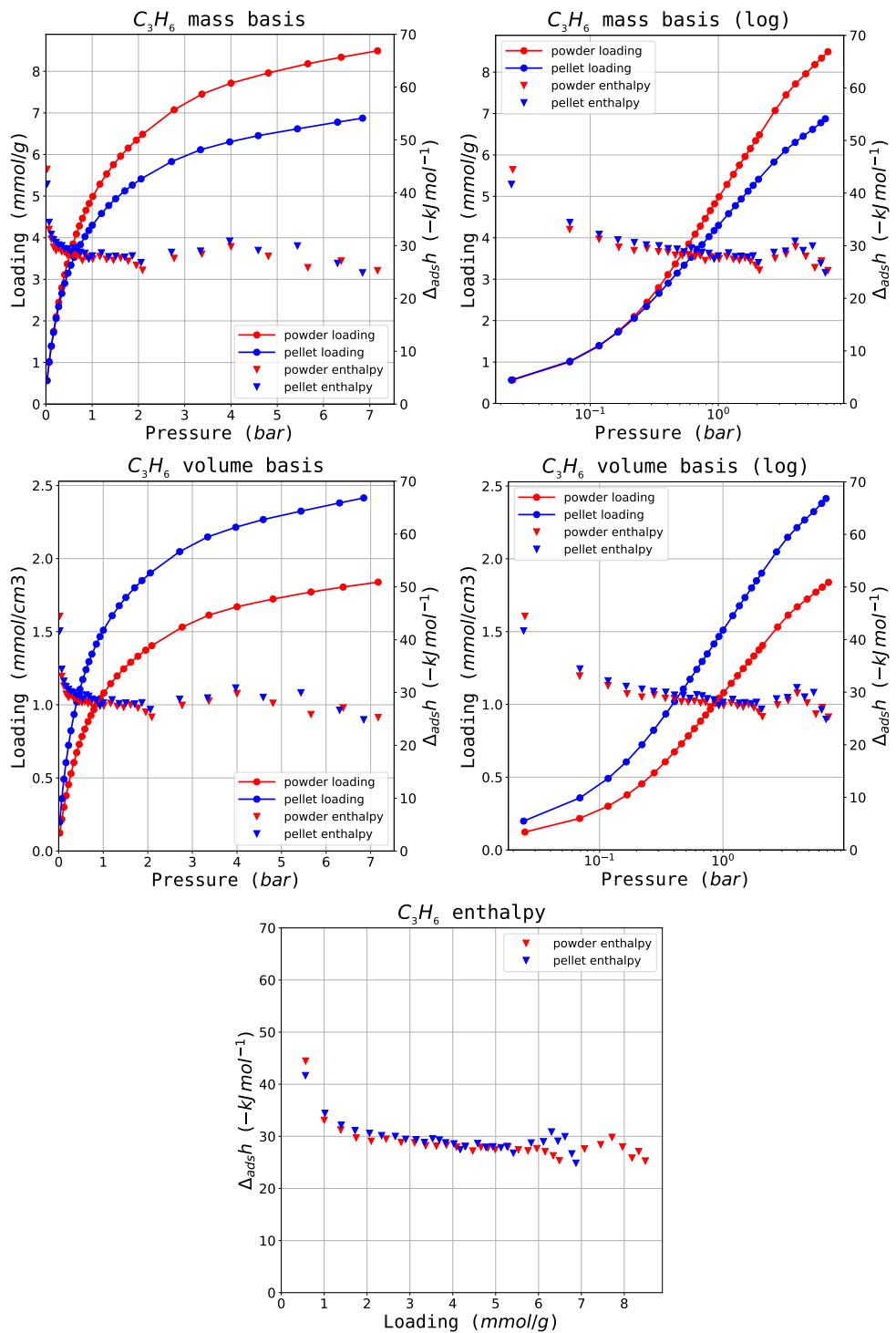


Fig. S18. Propylene calorimetric dataset for MIL-100(Fe)

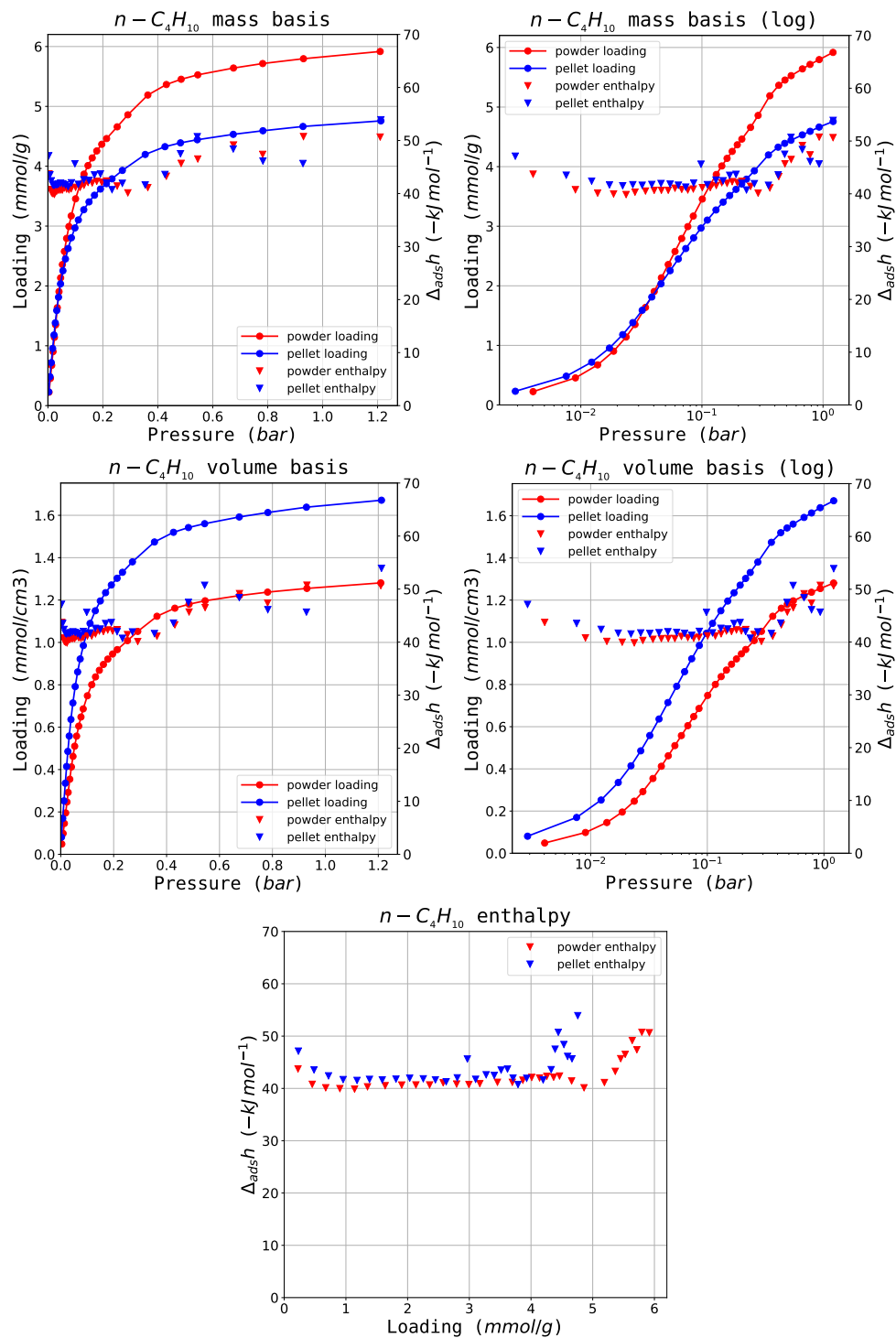


Fig. S19. Butane calorimetric dataset for MIL-100(Fe)

Calorimetry MIL-127(Fe)

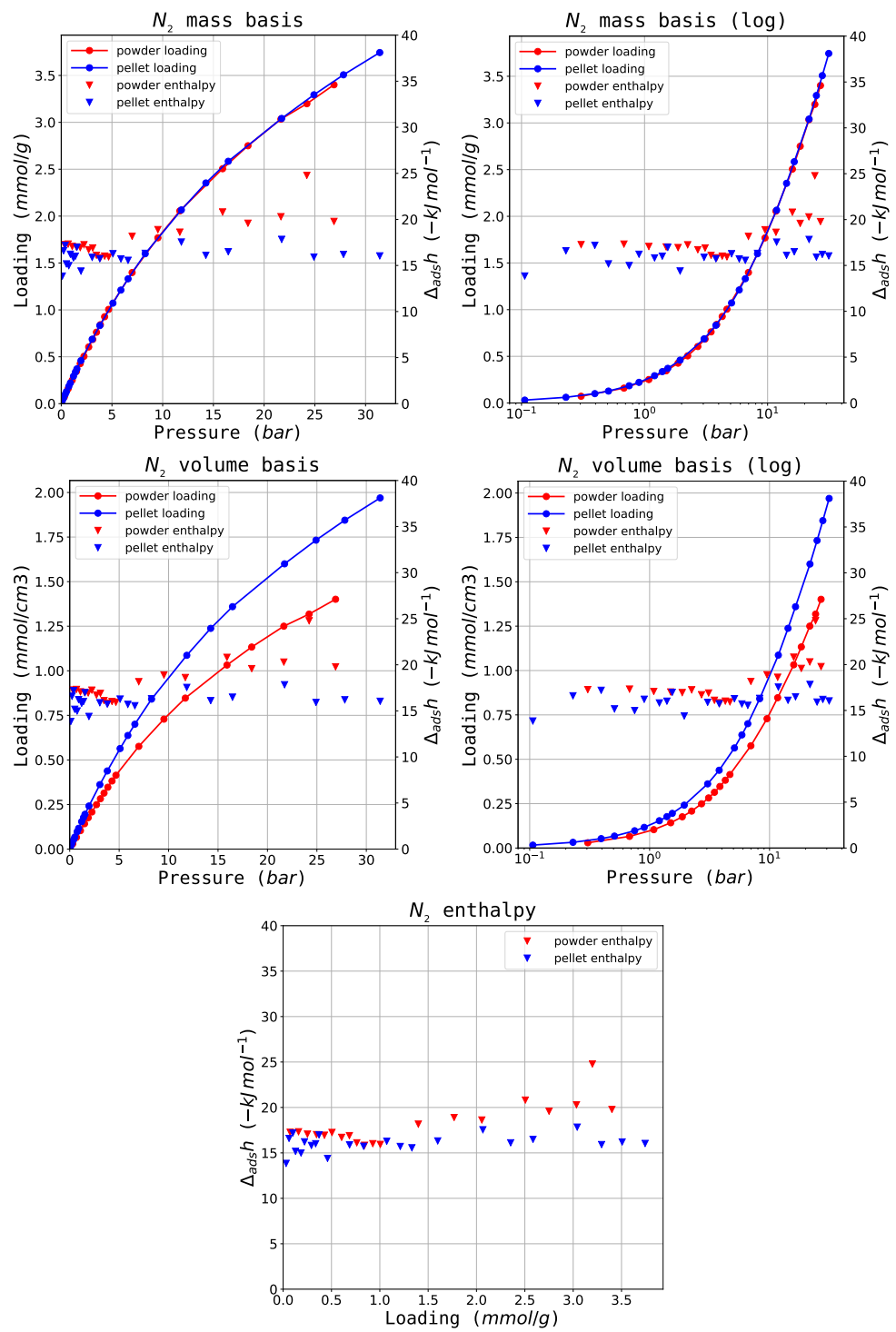


Fig. S20. Nitrogen calorimetric dataset for MIL-127(Fe)

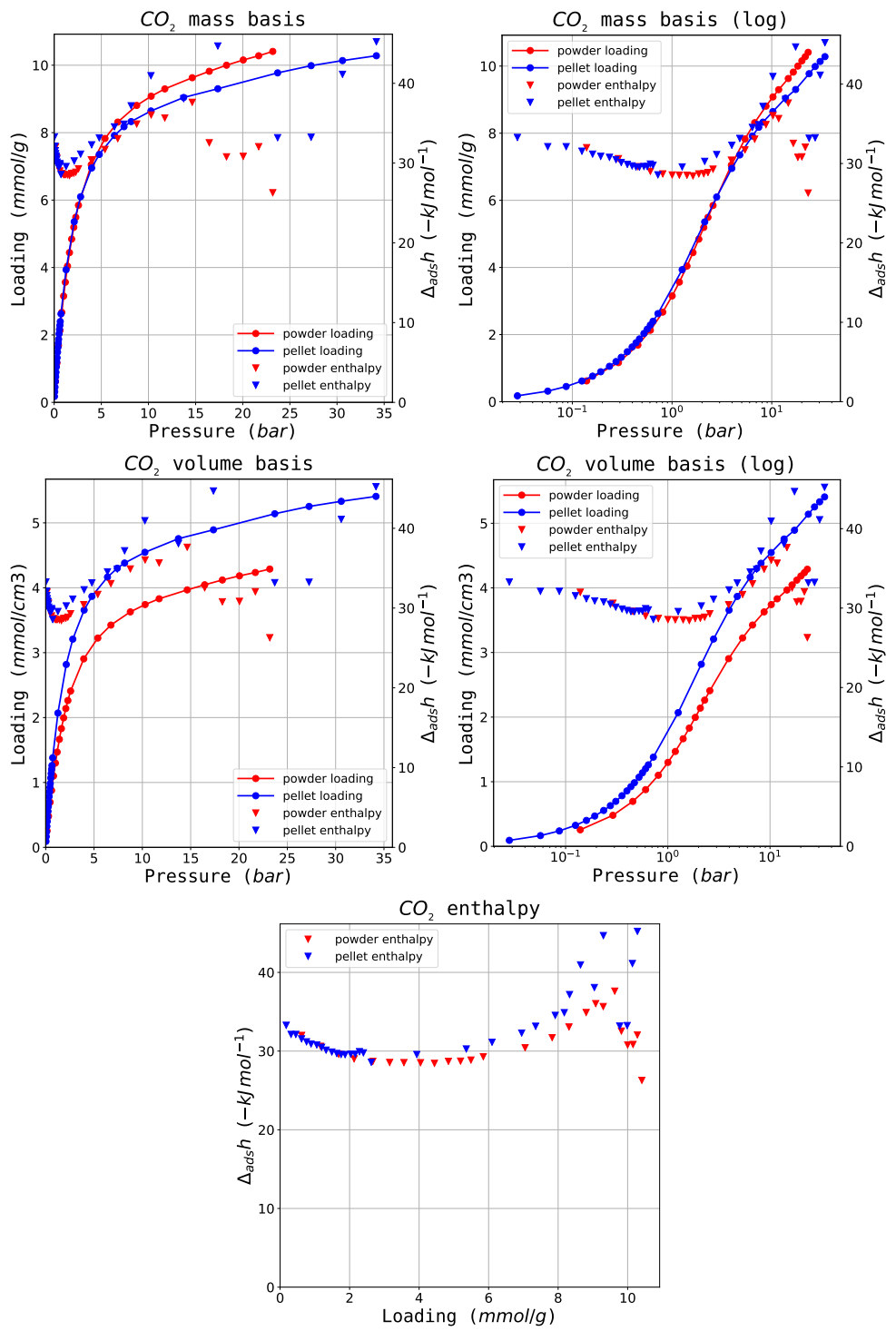


Fig. S21. Carbon dioxide calorimetric dataset for MIL-127(Fe)

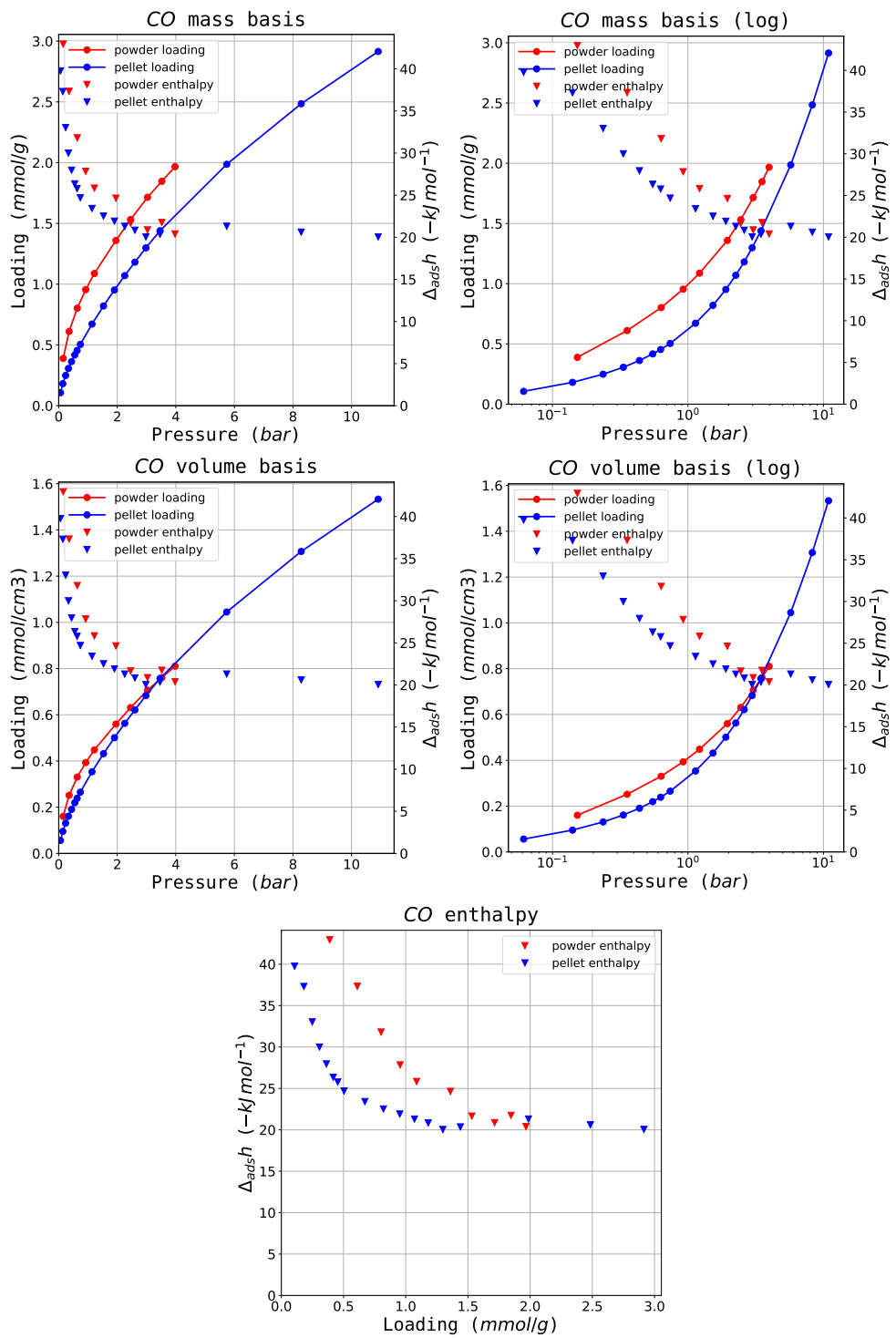


Fig. S22. Carbon monoxide calorimetric dataset for MIL-127(Fe)

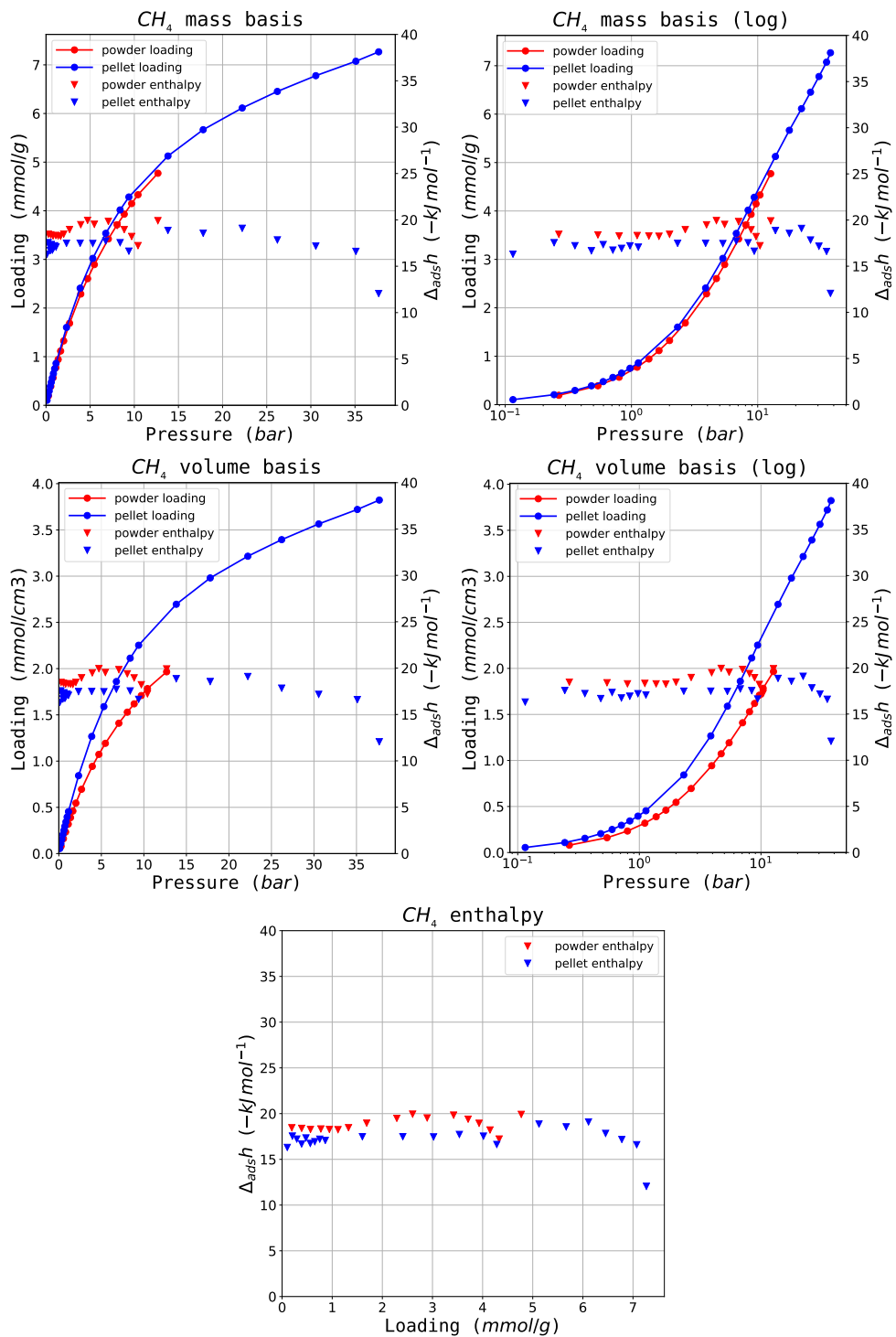


Fig. S23. Methane calorimetric dataset for MIL-127(Fe)

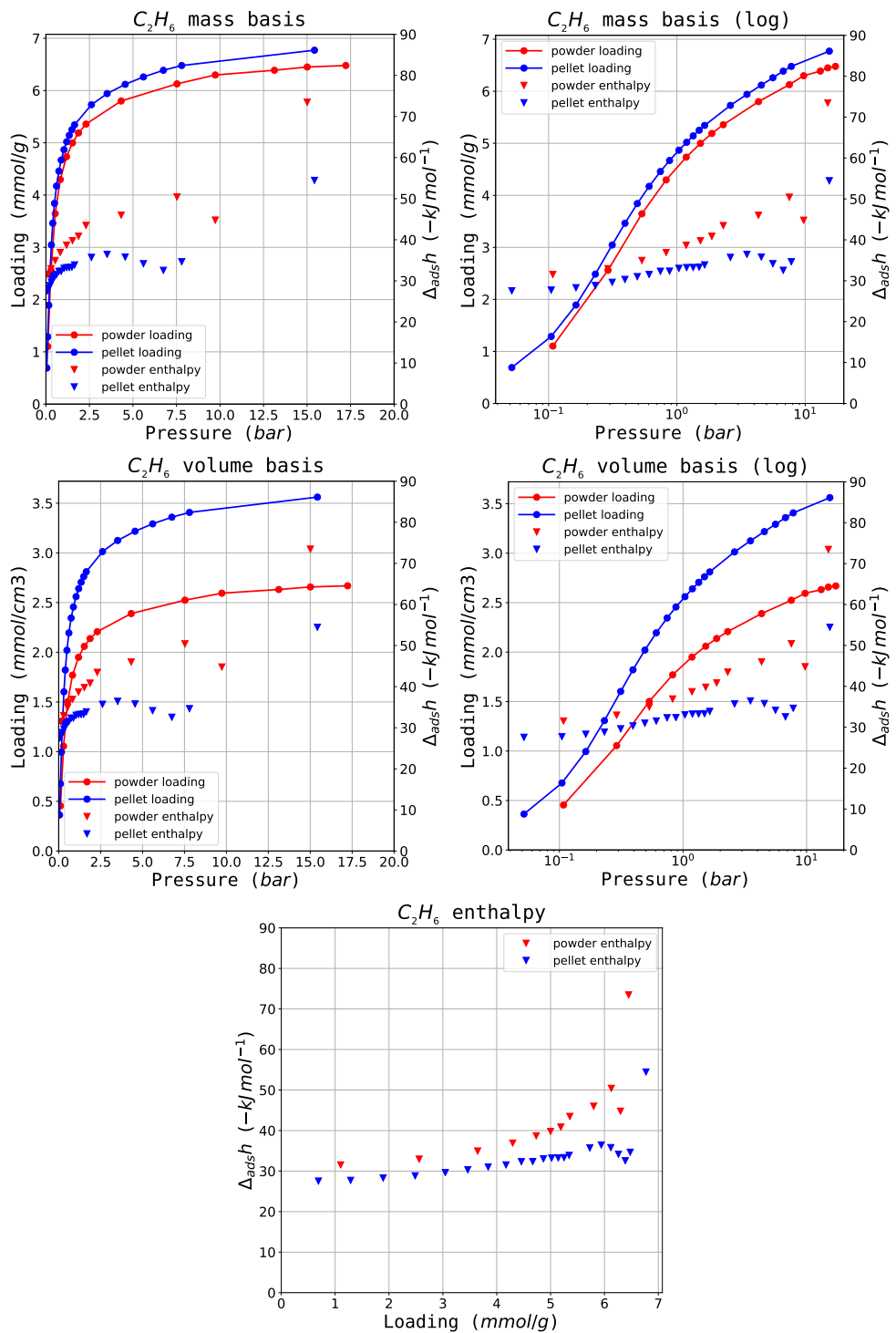


Fig. S24. Ethane calorimetric dataset for MIL-127(Fe)

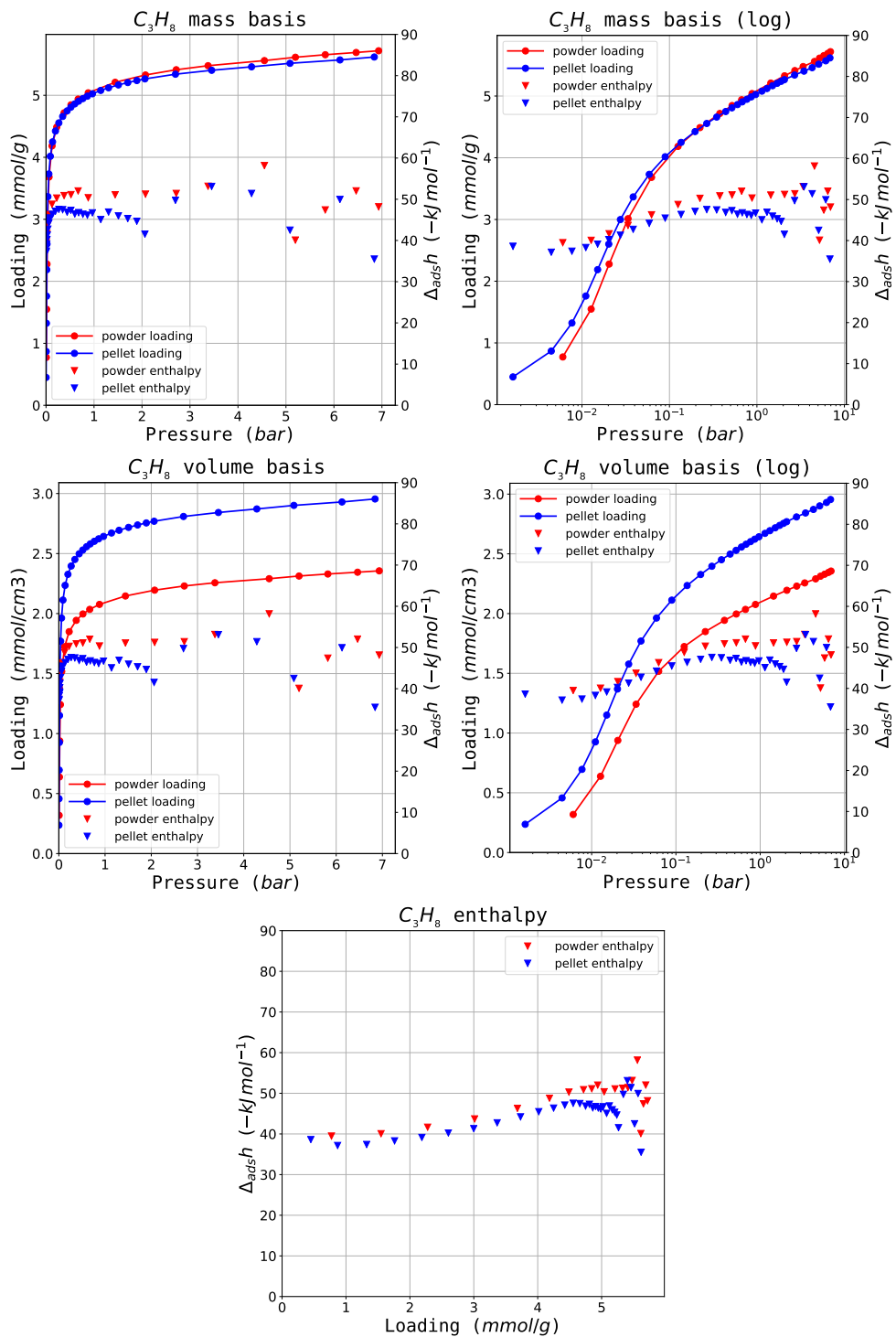


Fig. S25. Propane calorimetric dataset for MIL-127(Fe)

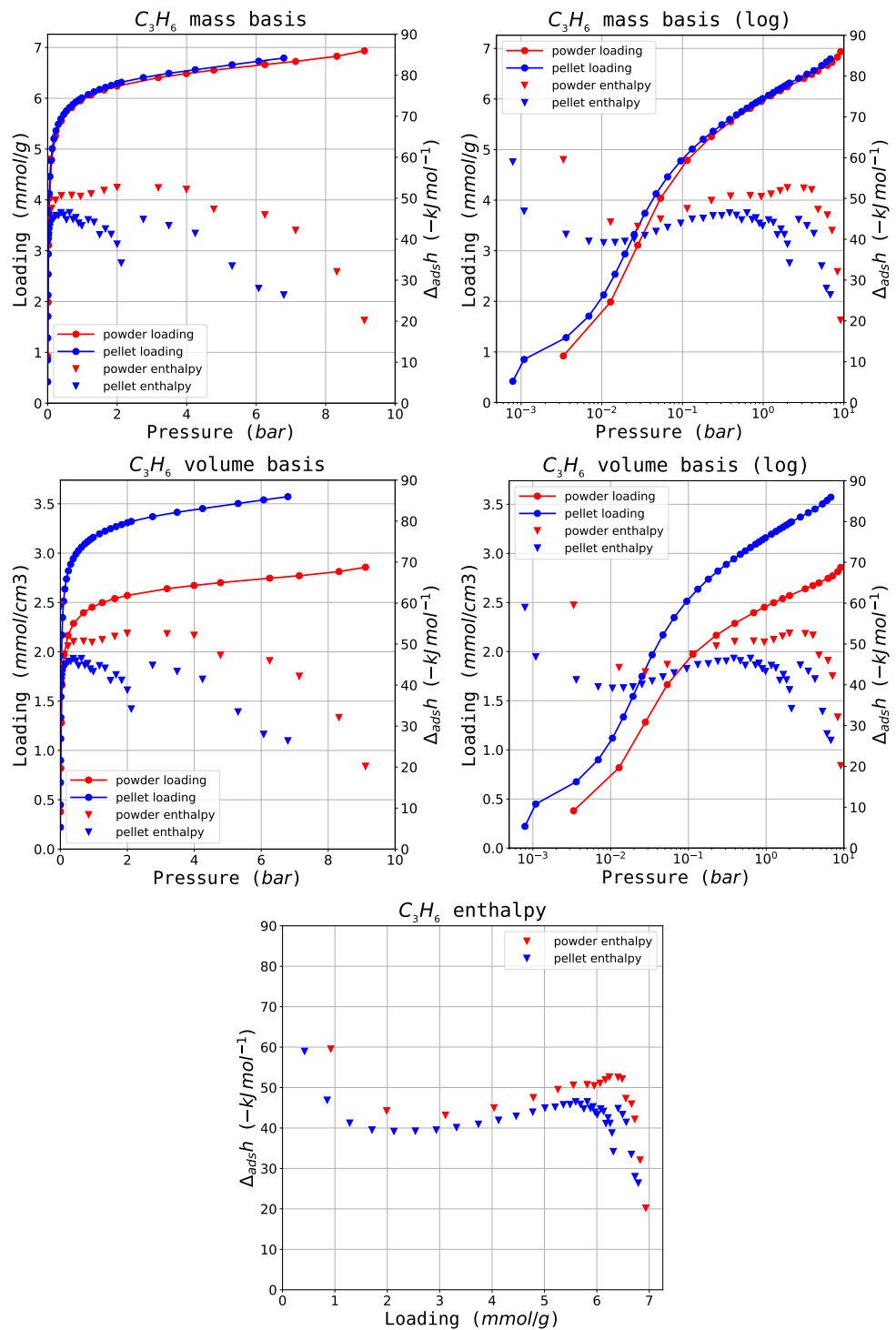


Fig. S26. Propylene calorimetric dataset for MIL-127(Fe)

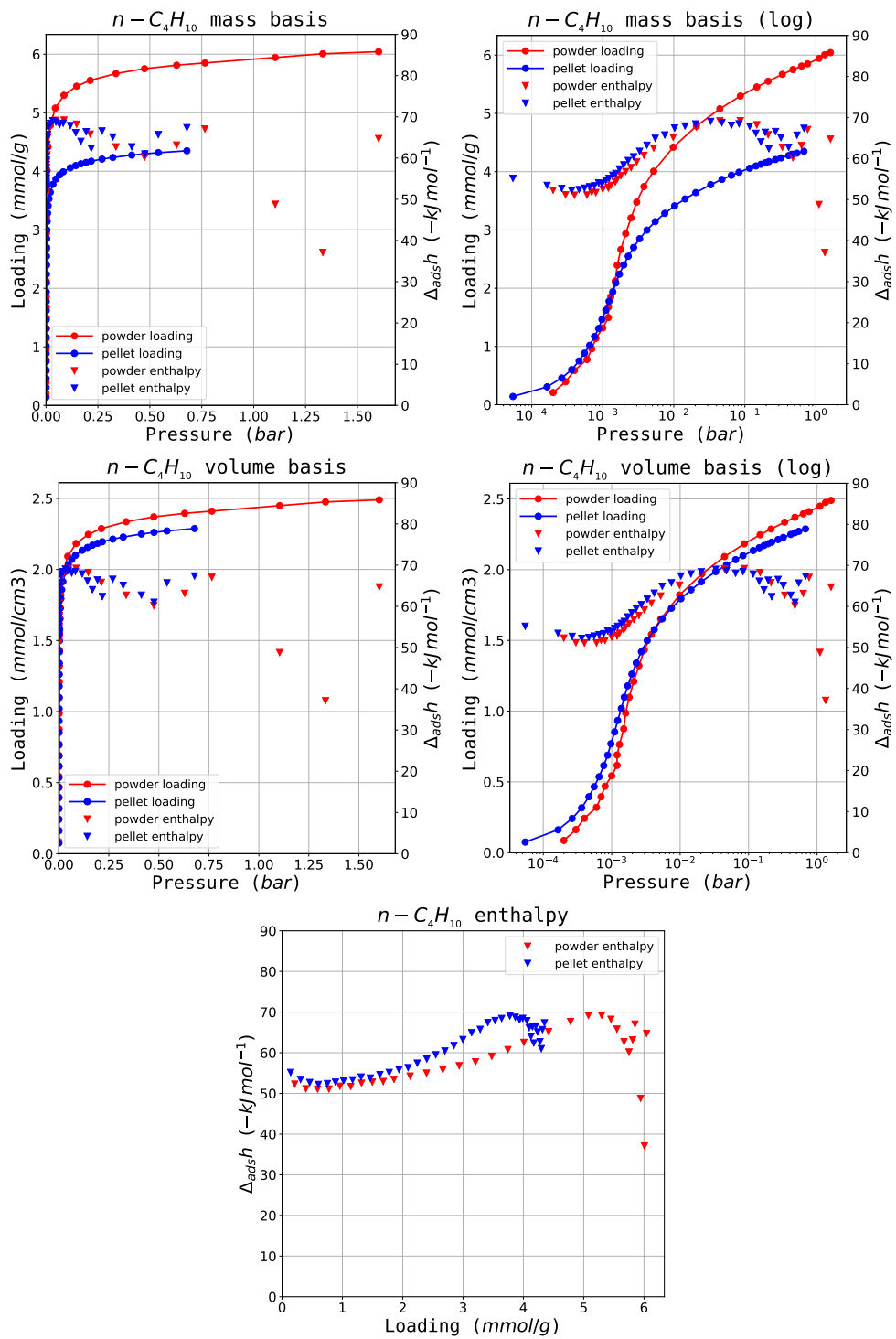


Fig. S27. Butane calorimetric dataset for MIL-127(Fe)

7. Water adsorption 298K dataset

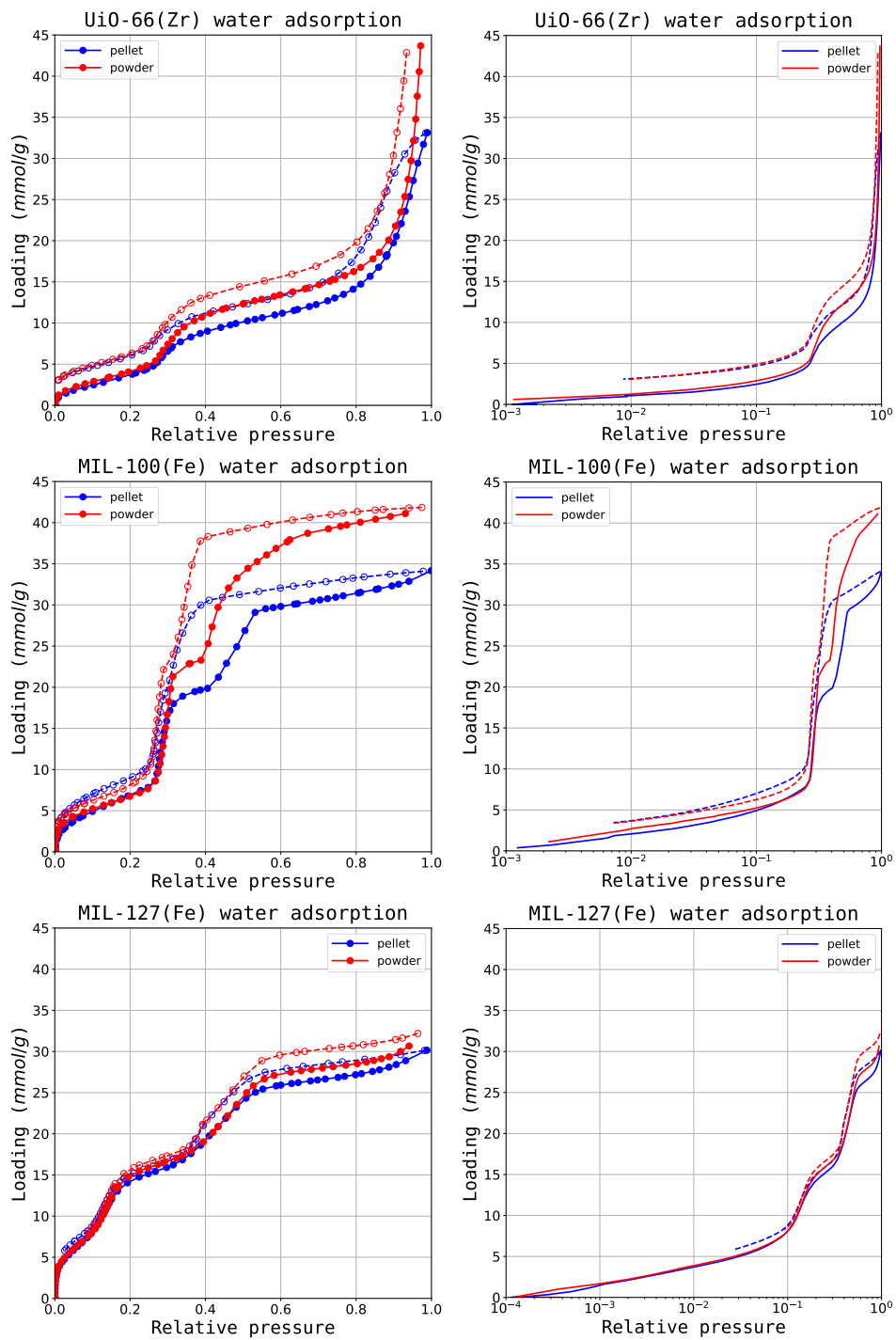


Fig. S28. Complete water adsorption isotherm dataset on materials

8. Methanol adsorption 298K dataset

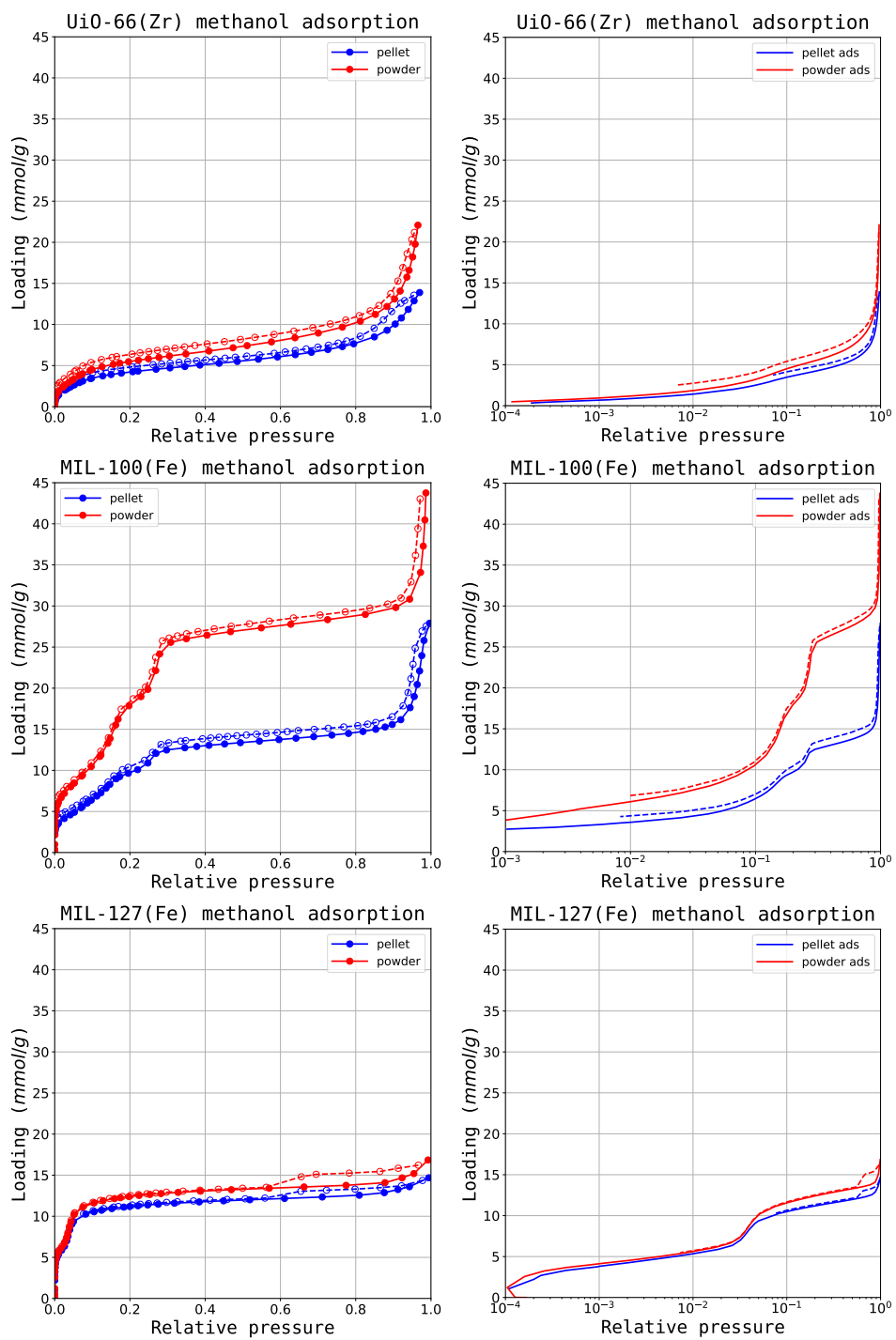


Fig. S29. Complete methanol adsorption isotherm dataset on materials

References

- (S1) F. Ragon, P. Horcajada, H. Chevreau, Y. K. Hwang, U.-H. Lee, S. R. Miller, T. Devic, J.-S. Chang and C. Serre, *Inorganic Chemistry*, 2014, **53**, 2491–2500.
- (S2) F. Jeremias, S. K. Henninger and C. Janiak, *Dalton Transactions*, 2016, **45**, 8637–8644.
- (S3) J. Rouquerol, F. Rouquerol, P. L. Llewellyn, G. Maurin and K. Sing, *Adsorption by Powders and Porous Solids : Principles, Methodology and Applications*, 2013.
- (S4) P. L. Llewellyn and G. Maurin, *Comptes Rendus Chimie*, 2005, **8**, 283–302.